Biogeochemical response of the Mediterranean Sea to the transient SRES–A2 climate change scenario

Camille Richon[1,*], Jean-Claude Dutay[1], Laurent Bopp[2], Briac Le Vu[2], James C. Orr[1], Samuel Somot[3], and François Dulac[1]

[1]LSCE/IPSL, Laboratoire des Sciences du Climat et de l'Environnement, CEA-CNRS-UVSQ, Gif-sur-Yvette, France
[2]Laboratoire de Météorologie Dynamique, LMD/IPSL, Ecole Normale Supérieure - PSL Research Univ., CNRS, Sorbonne Université, Ecole Polytechnique, Paris, France
[3]CNRM, Université de Toulouse, Météo-France, CNRS, Toulouse, France
[*]Now at: Department of Earth, Ocean and Ecological Sciences, School of Environmental Sciences, University of Liverpool, Liverpool L69 3GP, UK

Correspondence to: Camille Richon (crichon@liverpool.ac.uk)

Abstract. The Mediterranean region is a climate change hot-spot. Increasing greenhouse gas emissions are projected to lead to a significant warming of Mediterranean Sea waters, as well as major changes in its circulation, but the subsequent effects of such changes on marine biogeochemistry are still poorly understood. Our aim is to investigate the changes in nutrient concentrations and biological productivity in response to climate change in the Mediterranean region. To do so, we perform transient simulations with the coupled high resolution model NEMOMED8/PISCES using the high–emission IPCC SRES-A2 socio-economic scenario and corresponding Atlantic, Black Sea, and riverine nutrient inputs. Our results indicate that nitrate is accumulating in the Mediterranean Sea over the 21st century, whereas no tendency is found for phosphorus. These contrasted variations result from an unbalanced nitrogen–to–phosphorus input from fluxes through the Strait of Gibraltar and riverine discharge and lead to an expansion of phosphorus–limited regions across the Mediterranean. In addition, phytoplankton net primary productivity is reduced by 10 % in the 2090s in comparison to the present state, with reductions of up to 50 % in some regions such as the Aegean Sea as a result of nutrient limitation and vertical stratification. We also perform sensitivity tests in order to study separately the effects of climate and biogeochemical input changes on the Mediterranean future state. Our results show that changes in nutrient supply from the Strait of Gibraltar and from rivers and circulation changes linked to climate change may have opposing or synergistic effects on nutrient concentrations and surface primary productivity. In some regions such as the Adriatic Sea, half of the biogeochemical changes observed throughout the 21st century are linked with external nutrient input changes while the other half can be linked to climate change effects. This article is a first step in the study of transient climate change effects on the Mediterranean biogeochemistry, but calls for presently missing atmospheric deposition scenario and coordinated multi-model efforts to explore the various uncertainty sources of such a future projection.

1 Introduction

25   The Mediterranean basin is enclosed by three continents, with mountains, deserts, rivers, and indus-
trialized cities. This area is known as one of the most oligotrophic marine environment in the world
(Béthoux et al., 1998). Because of its high anthropogenic pressure and low biological productivity,
this region is predicted to be highly sensitive to future climate change impacts (Giorgi, 2006; Giorgi
and Lionello, 2008).

30   Records of the past evolution of the Mediterranean circulation show that the Mediterranean has un-
dergone abrupt changes in its circulation patterns over ancient times. In particular, high stratification
events, characterized by the preservation of organic matter in the sediment, known as sapropels,
have been recorded several times through geological history. The most recent was recorded 10 000
years ago and lasted about 3 000 years. This accumulation of organic matter in the sediments is

35   interpreted as the result of a strong stratification of the water column leading to suboxic deep lay-
ers (e.g. Rossignol-Strick et al., 1982; Rohling, 1991, 1994; Vadsaria et al., 2017). In more recent
times, abnormal winter conditions have led to changes in deep water formation, such as the East-
ern Mediterranean Transient (EMT) event that occurred during the early nineties and had chemical
impacts such as an increase in the Levantine basin salinity (see Theocharis et al., 1999; Lascaratos

40   et al., 1999; Nittis et al., 2003; Velaoras and Lascaratos, 2010; Roether et al., 2014). Also, changes
in the North Ionian Gyre circulation triggered the so–called Bimodal Oscillating System (BiOS) that
influenced phytoplankton bloom in the Ionian Sea through the modification of water transport that
led to modified nutrient distribution and altered local productivity (Civitarese et al., 2010). These
events show that a semi–enclosed basin with short residence time of water (around 100 years, see

45   Robinson et al., 2001) such as the Mediterranean is highly sensitive to climate conditions and that
perturbations of these conditions can modify the circulation, ultimately leading to changes in the
biogeochemistry.

Future climate projections with greenhouse gases high-emission scenarios yield an increase in tem-
perature and a decrease in precipitation over the Mediterranean region (Giorgi, 2006; IPCC, 2012)

50   leading to warmer and saltier seawater (Somot et al., 2006; Adloff et al., 2015). As a result of these
changes, the Mediterranean thermohaline circulation (MTHC) may significantly change with a con-
sistent weakening in the western basin and a less certain response in the eastern basin in climate
change scenarios characterized by high greenhouse gases emission (Somot et al., 2006; Adloff et al.,
2015). In all A2 runs, Adloff et al. (2015) show an increase in the stratification index at the end

55   of the 21st century. This will likely weaken the vertical mixing and may reduce nutrient supply in
the upper layer of the Mediterranean that is essential for phytoplankton to bloom (d'Ortenzio and
Ribera d'Alcalà, 2009; Herrmann et al., 2013; Auger et al., 2014).

Primary productivity in the ocean is influenced by water circulation and vertical mixing that brings
available nutrients to phytoplankton (Harley et al., 2006). Changes in oceanic physics such as mod-

60   ification of vertical mixing can have dramatic effects on plankton community dynamics and ulti-

mately on the productivity of the entire oceanic food web (Klein et al., 2003; Civitarese et al., 2010). Few studies have investigated the sensitivity of the oligotrophic Mediterranean Sea to future climate change (e.g. Herrmann et al., 2014, for the northwestern Mediterranean). Lazzari et al. (2014) investigated the effects of the A1B SRES (Special Report on Emissions Scenarios) moderate climate

65 change scenario on the Mediterranean biological productivity and plankton communities. They performed short (10–year) non–transient simulations at the beginning and the end of the 21st century and found a decreasing trend of phytoplankton biomass in response to this climate change scenario. Macias et al. (2015) simulated a "baseline" of expected consequences of climate change alone on the Mediterranean primary productivity. They found that according to the RCP 4.5 and RCP 8.5

70 scenarios, integrated primary productivity over the eastern Mediterranean basin may increase as a result of density changes (increased stratification isolating the upper layer from the rest of the water column). However, their results are based on non–transient simulations and present–day nutrient inputs. The response of the Mediterranean biogeochemistry to transient climate and biogeochemical change scenarios has never been evaluated.

75 Being a semi–enclosed oligotrophic basin, the Mediterranean is highly sensitive to external nutrient inputs. Their origins are mainly from coastal runoff, river discharge (Ludwig et al., 2009), Atlantic inputs through the Strait of Gibraltar (Gómez, 2003; Huertas et al., 2012), and atmospheric deposition (see e.g. Dulac et al., 1989; Christodoulaki et al., 2013; Gallisai et al., 2014; Guieu et al., 2014; Richon et al., 2017, 2018). Recent studies also showed that direct wastewater discharge (Powley

80 et al., 2016) and submarine groundwater (Rodellas et al., 2015) may be important sources of nutrient for the Mediterranean. However, these sources are to date not well quantified. This study aims at understanding the biogeochemical response of the Mediterranean to a "business–as–usual" climate change scenario throughout the 21st century. For this purpose, we use the high resolution coupled physical–biogeochemical model NEMOMED8/PISCES. We model the evolution of biogeochemical

85 tracers (nutrients, chlorophyll–a concentration, plankton biomass and primary production) under the SRES A2 climate change scenario for the 21st century (IPCC and Working Group III, 2000). The choice of the A2 scenario was driven by the availability of daily 3–D forcings for the biogeochemical model (physical forcings such as ocean currents, temperature and salinity, see Adloff et al., 2015). We are aware that using a single simulation will limit the robustness of our results. However the

90 computer power required to perform large ensembles with PISCES and the unavailability of 3-D daily ocean transient scenario data currently prevent a more extensive assessment.

This article is organized as follows: the coupled model, forcings and the different simulations are first described. We briefly evaluate the biogeochemical model in Section 3.1 and present the evolution of the physical and biogeochemical forcings in Section 3.2. In section 3.3, we expose the

95 temporal evolution of the main nutrients, their budgets in present and future conditions and discuss their impact on the biogeochemistry of the Mediterranean Sea in section 4.

2 Methods

2.1 The ocean model

The oceanic general circulation model used in this study is NEMO (Madec, 2008) in its regional
100   configuration for the Mediterranean Sea (NEMOMED8 Beuvier et al., 2010). The NEMOMED8
grid has a horizontal resolution of 1/8° stretched in latitude (i.e., with a resolution from 9 km in the
North to 12 km in the South of the domain). The model has 43 vertical levels with varying thick-
nesses (from 6 m in the surface layer to 200 m in the deepest layer). The Atlantic boundary is closed
at 11°W and tracers are introduced in a buffer zone between 11°W and 6°W.
105   Air–sea fluxes (momentum, heat, water) and river discharges used to force NEMOMED8 are pre-
scribed by the atmospheric Regional Climate Model ARPEGE–Climate (Déqué et al., 1994; Gibelin
and Déqué, 2003) using a global and stretched grid, which has a 50–km horizontal resolution over
the area of interest.

2.2 The SRES–A2 scenario simulation

110   ARPEGE–Climate is itself driven by greenhouse gases (GHG) and aerosol forcings following the
observations (up to year 2000) and the SRES–A2 scenario afterwards and by SST (Sea Surface Tem-
perature) coming from a previously run CNRM–CM coupled GCM (General Circulation Model)
simulation (Royer et al., 2002). In addition, the ocean component of CNRM–CM (a low resolution
NEMO version) provides the near–Atlantic conditions (3–D potential temperature and salinity) for
115   NEMOMED8. The various forcings and the modeling chain from the GCM to the ocean regional
model are described in details in Somot et al. (2006) and Adloff et al. (2015).

The NEMOMED8 simulation (ocean physics and forcings) used here corresponds to one of the sim-
ulations used and studied in Adloff et al. (2015), and more specifically the simulations labeled HIS
(historical period 1961 to 1999) and A2 (A2 scenario period 2000–2099) in their Table 1. This phys-
120   ical run has already been used to study climate change impacts on Mediterranean marine ecosystems
(Jordà et al., 2012; Hattab et al., 2014; Albouy et al., 2015; Andrello et al., 2015).

The main changes on the Mediterranean Sea physics (SST, SSS -Sea Surface Salinity-, surface circu-
lation, deep convection and thermohaline circulation, vertical stratification, sea level) are detailed in
Adloff et al. (2015). Briefly, changes in temperature and precipitation in the A2 scenario lead to in-
125   creased evaporation in the basin at the end of the 21st century. Freshwater inputs from rivers and the
Black Sea decrease along with total precipitation. This consequently leads to a significant increase in
net transport through the Strait of Gibraltar (+0.018 Sv by the end of the century). Temperature and
salinity increase strongly, leading to a decrease in surface density and an overall increase in vertical
stratification. Average sea surface temperature of the Mediterranean rises by up to 3°C by the end
130   of the century. However, the temperature rise is not homogeneous in the basin, regions such as the
Balearic, Aegean, Levantine and North Ionian undergo a more intense warming (over 3.4 °C) prob-

4

ably due to the addition of the atmosphere-originated quasi-homogeneous warming with the local effect of surface current changes. The salinity increases by 0.5 (practical salinity units) on average across the basin.

135 In the A2 simulation, the entire Mediterranean basin is projected to become more stratified by 2100 and deep water formation is generally reduced. These variations in hydrological characteristics of the water masses generate important changes in the circulation and in particular in the vertical mixing intensity. The strong reduction in vertical mixing observed in all deep water formation areas of the basin is linked with the changes in salinity and temperature of the water masses.

140 **2.3   The biogeochemical model**

Here, the physical model NEMOMED8 is coupled to the biogeochemical model PISCES (Aumont and Bopp, 2006), already used for investigations in the Mediterranean basin (Richon et al., 2017, 2018). This Monod–type model (Monod, 1958) has 24 biogeochemical compartments including 2 phytoplankton (nanophytoplankton and diatoms) and 2 zooplankton size classes (microzooplank-

145 ton and mesozooplankton). Phytoplankton growth is limited by the external concentration of five different nutrients: nitrate, ammonium, phosphate, silicic acid and iron. In this version of PISCES, elemental ratios of C:N:P in the organic matter are fixed to 122:16:1 following Takahashi et al. (1985). There is no explicit bacterial compartment but bacterial biomass is calculated using zooplankton biomass (see Aumont and Bopp, 2006, for details). Organic matter is divided in 2 forms:

150 dissolved organic carbon (DOC) and particulate organic carbon. The biogeochemical model is ran in offline mode (see e.g. Palmieri et al., 2015): biogeochemical quantities are passive tracers, they are transported following an advection–diffusion equation using dynamical fields (velocities, mixing coefficients...) calculated beforehand in a separate simulation with only the dynamical model NEMOMED8.

155 **2.4   Boundary and initial physical and biogeochemical conditions**

External nutrient supply for the biogeochemical model include inputs from the Atlantic Ocean and from Mediterranean rivers. We did not include atmospheric deposition as there is currently no scenario for its future evolution. Similarly, we did not include submarine groundwater discharge and direct wastewater discharge as there is to date no climatology for these sources. Atlantic input is pre-

160 scribed from water exchange through the Strait of Gibraltar in the NEMO circulation model along with the concentrations of biogeochemical tracers in the buffer zone. Nutrient concentrations in the buffer zone are prescribed from a global ocean climate projection using the A2 simulation values from IPSL–CM5–LR (Dufresne et al., 2013) performed within the framework of the CMIP5 project (Taylor et al., 2012). Nutrient concentrations in the buffer–zone are relaxed to these values with a

165 time constant of one month.
Nutrients input from rivers are derived from Ludwig et al. (2010) before 2000, Dissolved inorganic

5

carbon (DIC) and Si are derived from Ludwig et al. (2009). For the 21st century, we use the estimations for nutrient discharge proposed by Ludwig et al. (2010) of the "Order from Strength" scenario from the Millenium Ecosystem Assessment (MEA) (Cork et al., 2005), which gives nitrate and phos-

170 phate discharge per sub–basin in 2030 and 2050. Yearly values are obtained by linear interpolation between 2000 and 2030 and between 2030 and 2050, after which they are held constant until the end of the simulation in 2100. Seasonal variability coming from four of the largest rivers for Mediterranean and Black Sea (Rhône, Po, Ebro and Danube) is also included. According to Ludwig et al. (2010), the future trends in nutrient discharge from the major rivers of the Mediterranean stay within

175 the interannual variability over the past 40 years. This scenario is based on hypotheses of very little efforts made towards mitigation of climate change. Ludwig et al. (2010) point out some substantial changes in the nutrient and water budget in specific regions. However, total riverine nutrient input is not drastically changed at the basin scale. In particular, according to their scenario, the northern part of the Mediterranean has decreasing trends in nitrate discharge whereas it is increasing in the

180 southeastern Levantine. Freshwater discharge from Ludwig et al. (2010) is based on the SESAME model reconstruction and differs from the ARPEGE–Climate model used here. This may lead to incoherences between water and nutrient discharges, but the nutrient discharges from Ludwig et al. (2010) are the only available values, and the SESAME model is not coupled with NEMO/PISCES. Adloff et al. (2015) evaluate the changes in total freshwater runoff in the HIS/A2 simulation. Their

185 Table 2 shows that the total freshwater runoff to the Mediterranean is lower than the Ludwig et al. (2009) estimate (by about 30 %). They found approximately 27 % decrease in total runoff by the end of the 21st century. This trend is consistent with the deceasing trend found by Ludwig et al. (2010). However, the 2050 estimates of freshwater runoff from Ludwig et al. (2010) are only 13 % lower than the 1970 and 2000 estimates. The freshwater runoff decrease in the physical model is more

190 important than in the nutrient runoff model. This may result in higher nutrient concentrations at the river mouth. We are also aware that the future evolution of river discharges into the Mediterranean Sea is highly uncertain and depends at least on the scenario choice and on the model and modelling strategy choice (Sanchez-Gomez et al., 2009; Dubois et al., 2012; Adloff et al., 2015). However, nutrients from river discharge are consumed rapidly at proximity of the river mouth and we believe

195 these potential higher concentrations don't have a large impact of the results.

Initial nutrient concentrations in the Mediterranean come from the SeaDataNet database (Schaap and Lowry, 2010) and initial nutrient concentrations in the buffer zone are prescribed from the World Ocean Atlas (WOA) (Locarnini et al., 2006). Salinity and temperature are initialized from the MEDATLAS II climatology of Fichaut et al. (2003).

200 All simulations begin from a restart of a historical run starting in January 1965 following a spin–up of more than 115 years done with a loop of the period 1966 to 1981 for the physical forcings and the river nutrient discharge.

2.5 Simulation set–up

All simulations are performed for 120 years. The control run CTRL is performed with forcing con-
ditions corresponding to the 1966–1981 period looped over the simulation period. This period was
chosen in order to avoid including in the CTRL years with too important warming such as the 1980s
and 1990s. The scenario simulation is referred to as HIS/A2 as in Adloff et al. (2015). HIS is the
name of the historical period (in our case between 1980 and 1999), and A2 is the name of the 2000–
2099 scenario simulation.

In order to quantify separately the effects of climate and biogeochemical changes, we performed
2 additional control simulations: CTRL_R with climatic and Atlantic conditions corresponding to
present–day conditions and river nutrient discharge following the scenario evolution, and CTRL_RG
with climatic conditions corresponding to present–day conditions, and river nutrient discharge and
Atlantic buffer–zone concentrations following the scenario conditions. Table 1 describes the different
simulations. The effects of nutrient inputs from exchanges through the Strait of Gibraltar and riverine
discharge independent of climate effect are derived by CTRL_R minus CTRL and CTRL_RG minus
CTRL_R. Similarly, to derive the effects of climate change and nutrient input change on nutrient
budgets, we use the difference between HIS/A2 and CTRL. To derive the effects of climate change
only, we calculate the difference between HIS/A2 and CTRL_RG.

3 Results

3.1 Evaluation of the NEMOMED8/PISCES model

NEMOMED8 has already been used in a number of regional Mediterranean Sea modeling studies
either in hindcast mode (Beuvier et al., 2010; Herrmann et al., 2010; Sevault et al., 2014; Soto-
Navarro et al., 2015; Dunić et al., 2016) or scenario mode (Adloff et al., 2015). It produces the main
characteristics of the Mediterranean Sea circulation. Evaluation of the HIS simulation provided in
Adloff et al. (2015) shows that the main physical characteristics of the Mediterranean are produced,
in spite of a too cold upper layer (1°C colder than observations) and too little stratification in com-
parison to observations. In particular, the HIS simulation matches closely the observed thermohaline
circulation in the Adriatic and Ionian basins (see Adloff et al., 2015).

The regional NEMOMED physical model has already been coupled to the biogeochemical model
PISCES on a 1/12° grid horizontal resolution (Palmieri et al., 2015; Richon et al., 2017, 2018), but
no future climate simulation has yet been performed. As a first study coupling NEMOMED8 with
PISCES, we compared the main biogeochemical features of our simulations with available data. Fig-
ure 1 shows the surface average chlorophyll concentrations in the top 10 meters of the CTRL and
HIS/A2 simulations, and from satellite estimations from MyOcean Dataset (http://marine.copernicus.eu).
All chlorophyll values in the article and the data are chlorophyll–a. The model correctly reproduces

the main high–chlorophyll regions such as the Gulf of Lions and coastal areas. However, Figure 1 shows an underestimation of about 50 % of the surface chlorophyll concentrations by the model in these productive areas. The west–to–east gradient of productivity is also reproduced by the model with values that agree with satellite estimates. Moreover, this Figure shows that chlorophyll produced by the CTRL is stable over time. The model fails, however, to reproduce the observed chlorophyll– rich areas in the Gulf of Gabes and at the mouth of the Nile. This discrepancy is probably linked with insufficient simulated nutrient discharge from coastal runoff in these regions. Moreover, several studies (see e.g. Claustre et al., 2002; Morel and Gentili, 2009) show that satellite estimates have a systematic positive bias in the coastal regions because of the high concentrations of colored dissolved organic matter and the presence of dust particles in seawater back scattering light. Figure 2 provides an evaluation of the average chlorophyll surface concentration evolution over the entire basin for the period 1997–2005. This Figure shows that the normalized chlorophyll surface concentration in the model is close to the estimates provided by the SeaWiFs satellite data (Bosc et al., 2004). Even though the interannual variability of the model is 50 % smaller than in the satellite product, the model captures the increase in chlorophyll concentration between 2002 and 2005 (approximately 15 % of increase in the model and 30 % in the satellite data). The evaluation of the model against 2 independent datasets shows that the model yields satisfying estimates of surface chlorophyll.

The vertical distribution of nitrate and phosphate over a section crossing the Mediterranean from East to West as well as chlorophyll and nutrient concentration profiles at the DYFAMED station are shown in appendix (Figures A1 and A3). These figures show that the model produces some seasonal and interanuual variability of the nutricline depth and intensity. However, the nutricline depth and DCM depth are consistently overestimated by the model in comparison to the data. The nutricline intensities seem to be underestimated by about 50 % and the depth is overestimated. However, nutricline depth deepens from 100–120 m to 180–200 m between the western and the eastern basins (see Figure A3).

In spite of some underestimation of nutrient concentrations that are probably linked with the features of the simulated intermediate and deep waters characteristics, the PISCES model reproduces the main characteristics of the Mediterranean biogeochemistry, including a salient west–to–east gradient in nutrient concentrations, low surface nutrient concentrations and a deep chlorophyll maximum (DCM). The average chlorophyll concentration observed at the DYFAMED station in the top 200 m is $233 \pm 146 \, 10^{-9} \mathrm{g \, L^{-1}}$ (average over the 1991–2005 period), while the model value for the HIS/A2 simulation over the same period is $159 \pm 87 \, 10^{-9} \mathrm{g \, L^{-1}}$. These performances lend credence to our efforts to investigate the evolution of the Mediterranean biogeochemistry under the A2 climate change scenario with the same modeling platform.

3.2 Evolution of temperature and salinity

Average surface temperature and salinity (SST and SSS) evolution in the entire basin during the CTRL and HIS/A2 simulations are shown in Figure 3, which confirms results from Adloff et al. (2015) and shows that the CTRL simulation is stable over time. Beyond this basin–wide average variation in SST and SSS, a more detailed analysis reveals much greater variability depending on the region (Somot et al., 2006; Adloff et al., 2015). For instance, the Balearic Sea is more sensitive to warming than the rest of the western basin, and the eastern basin has a more intense warming than the western basin (up to 3°C warming in the eastern basin and in the Balearic Sea). Also, the surface salinity in the Aegean Sea increases more than the other regions.

3.3 Evolution of the nutrient budgets in the Mediterranean Sea

The nutrient budgets of the semi–enclosed Mediterranean basin are highly dependent on external sources (e.g. Ludwig et al., 2009, 2010; Huertas et al., 2012; Christodoulaki et al., 2013). In order to map the effects of climate change on the Mediterranean nutrient balance, we calculated mass budgets of inorganic nitrate and phosphate during the simulated period. These budgets take into account changes in Atlantic input, river discharge and sedimentation. Nitrate can also accumulate in the Mediterranean waters through N_2 fixation by cyanobacteria, but this process accounts for less than 1 % of the total nitrate budget (Ibello et al., 2010; Bonnet et al., 2011; Yogev et al., 2011), and is neglected here.

In this Section, we refer to the period 1980-1999 as the beginning of the century, to the period 2030–2049 as the middle of the century and to the period 2080–2099 as the end of the century. Also, we derive the effects of river input changes as the difference of nutrient concentrations between CTRL_R and CTRL over these time periods. Similarly, the effects of changes in nutrient fluxes through the Strait of Gibraltar are derived by the differences between CTRL_RG and CTRL_R, and the effects of climate change by the difference between HIS/A2 and CTRL_RG.

3.3.1 Phosphate and nitrate budgets under climate and biogeochemical changes in the Mediterranean

Tables 2 and 3 summarize the average phosphate and nitrate content in all simulations for the 3 time periods described earlier.

Phosphate content in the entire Mediterranean has increased in our simulation by 6 % over the 21st century, as determined by the difference between CTRL and HIS/A2 simulations between 1980-1999 and 2080–2099. The increase is more important in the eastern basin than in the western basin.

9

305   In particular, we observe an 8 % increase in phosphate content in the Ionian–Levantine sub–basin in 2080–2099 compared to 1980–1999. The effects of phosphate river input changes are substantial over the first half of the century. We observe 3 % decrease in phosphate content in the entire Mediterranean between 1980–1999 and 2030–2049 due to river input changes (difference between CTRL_R and CTRL). Changes in phosphate fluxes thought the Strait of Gibraltar seem to have lim-

310   ited effect on the global Mediterranean phosphate content. However, climate change effects lead to a global enhancement of 10 % in phosphate content in 2080–2099 in comparison to 1980–1999. This result shows contrasted effects of physical and biogeochemical conditions on the evolution of nutrient concentrations.

315   Table 3 shows that in the model, the combined effects of climate, riverine and Atlantic nutrients input changes over the 21st century lead to a 17 % increase in nitrate content over the Mediterranean in the 2080–2099 period compared to 1980–1999 (derived from the calculation of HIS/A2–CTRL). Changes in river discharge in the Mediterranean over the century lead to 9 % enhancement of nitrate content by the end of the century (2080–2099) compared to the beginning of the simulation period

320   (1980–1999). The most important effects of river input changes are observed in the Adriatic basin (over 50 % nitrate accumulation by the end of the century). Over the entire Mediterranean, the effects of changes in the fluxes though the Strait of Gibraltar on nitrate content are weak (< 1 %). However, the comparison of nitrate content in CTRL_R and CTRL_RG in the western basin shows a 3 % decrease in nitrate content in the western basin during the 2030–2049 period followed by an

325   increase resulting in +1 % nitrate by 2080–2099 compared to the 1980–1999 period. Finally, climate change effects lead to 7 % increase in nitrate content over the Mediterranean basin in the 2080–2099 period compared to 1980–1999 (computed by HIS/A2–CTRL_RG). These results indicate that river inputs and climate change are the main drivers of nitrate content changes in the Mediterranean basin over the 21st century.

330   **3.3.2   Fluxes of nutrients through the Strait of Gibraltar**

The Mediterranean is connected to the global ocean by the narrow Strait of Gibraltar. Water masses transport through this strait contributes substantially to its water and nutrient budgets (e.g. Gómez, 2003; Huertas et al., 2012). The Mediterranean is a remineralization basin that has net negative fluxes of inorganic nutrients (i.e. organic nutrients enter the basin through the Gibraltar Strait surface wa-

335   ters and inorganic nutrient leave the Mediterranean through the deep waters of the Gibraltar Strait Huertas et al., 2012). Figure 4 shows the evolution of incoming and outgoing nitrate and phosphate fluxes through the Strait of Gibraltar in the HIS/A2 and in the CTRL simulations. We observe similar trends in phosphate and nitrate fluxes in the model. This is linked to the Redfieldian behavior of the primary production in PISCES. According to the HIS/A2 simulation, the incoming fluxes of nitrate

340   and phosphate decrease slightly (from 50 the 35 Gmol month^{-1} for nitrate and from 2.5 to 1.55

Gmol month^{-1} for phosphate) until the middle of the century (with a period of increased incoming fluxes of both phosphate and nitrate in the 1990s) and then increase to reach values higher than the control in the last 25 years of simulations (Figure 4). Outgoing fluxes follow the same trends as incoming fluxes: total outgoing nitrate and phosphate fluxes decrease from 1980 to 2040 (flux values
345　getting closer to zero) and then increase until the end of the century. We observe a decreasing trend in the nitrate outgoing flux in the control (from -129 to -110 Gmol month^{-1} representing about 18 %). At the end of the 21st century, incoming fluxes of nutrients have increased in the scenario simulation by about 13 % (difference between the 2080–2099 and 1980–1999 periods). But this significant increase (linear regression reveals a positive slope with correlation coefficient greater than 0.75 and
350　p–value < 0.001 for the second half of the simulation period for both nitrate and phosphate) follows a decrease of over 20 % in incoming nutrient fluxes between the 1980–1999 and the 2030–2049 periods. Most of the decrease is observed between 2030 and 2040 (decrease of 15 and 1 Gmol month^{-1} for nitrate and phosphate respectively during this decade). Outgoing fluxes increase less between the beginning and the end of the century (3.5 and 3.9 % for phosphate and nitrate respectively, Fig-
355　ure 4). If the relative changes in incoming and outgoing fluxes seem to indicate an increase in the net incoming flux, the absolute values seem to show a rather steady net flux between the beginning and the end of the century. Net flux at the beginning of the century is around -83 Gmol month^{-1} for nitrate and -3 Gmol month^{-1} for phosphate. At the end of the century, the fluxes are about -80 Gmol month^{-1} and -2.5 Gmol month^{-1} for nitrate and phosphate respectively. Also, these net fluxes
360　are close to the CTRL net fluxes. These trends result from the evolution of water fluxes through the Strait of Gibraltar computed by NEMOMED8 and the A2 scenario of nutrient concentrations in the buffer zone taken from Dufresne et al. (2013).

The imbalance between incoming and outgoing nutrient flux anomalies may be a cause for the observed accumulation of inorganic nutrients (in particular of nitrate) in the basin.

365　### 3.3.3　River fluxes of nutrients

River discharge is the main external source of phosphate for the eastern part of the basin (Krom et al., 2004; Christodoulaki et al., 2013). Figure 5 shows the total discharge of phosphate and nitrate from rivers to the Mediterranean Sea.

370　Phosphate discharge decreases by 25 % between the beginning and the end of the simulation period. As suggested by Ludwig et al. (2010), phosphate discharge in the A2 period stays lower than in the HIS period, in spite of a small discharge enhancement between 2030 and 2049.

Nitrate discharge in the HIS/A2 simulation is significantly higher than in CTRL (between 30 and 60 Gmol month^{-1} difference). Nitrate total discharge in the Mediterranean has continuously increased
375　from the 1960s (see the CTRL values for the years 1966–1981). According to the HIS/A2 simulation, total river nitrate discharge is 24 % larger during 2080-2099 than during 1980-1999.

11

3.3.4 Sedimentation

Sedimentation removes nutrients from the Mediterranean Sea. In this version of PISCES, the loss of nitrogen and phosphorus to the sediment is calculated from the sinking of organic carbon particles to
380 the sediment (linked through the Redfield ratio). Sediment fluxes of phosphorus and nitrogen during the simulations are shown in Figure 6.

The loss to the sediment decreases rapidly during the HIS simulation (1980–1999). By the end of the 21st century, sedimentation of P and N are almost 50 % lower relative to the 1980 fluxes.
385

3.3.5 Evolution of phosphate and nitrate concentrations

In order to observe the general evolution of nutrient concentrations over the 21st century, we plotted the evolution of phosphate and nitrate concentrations for the entire simulation period in the western and eastern basins. The separation between western and eastern basin is the Sicily Strait. Therefore,
390 the eastern basin includes the Ionian, Levantine, Adriatic and Aegean basins. Figure 7 shows the evolution of average phosphate concentrations in the western and eastern basin, respectively, for the surface (0–200 m), intermediate (200–600 m) and bottom (> 600 m) layers of the water column.

Figures 7a and 4b show that the evolution of surface phosphate concentration in the western basin
395 is linked with phosphate inputs through the Strait of Gibraltar (Pearson's correlation coefficient is 0.85, p–value < 1 %). We observe that phosphate concentration in HIS/A2 decreases in the surface and intermediate layers of the western basin until the middle of the century (concentration decreases by about 0.015 mmol m^{-3} in the surface layer and by 0.017 mmol m^{-3} in the intermediate layer) and then increases again until the end of the century to reach similar concentration than
400 in 1980 in the surface layer and higher concentrations than in 1980 in the intermediate layer (about 0.01 mmol m^{-3} higher). This evolution is different than the controls. Figure 7a shows that the difference in phosphate concentrations in the surface layer of the western Mediterranean in the CTRL_RG and CTRL_R simulations is important only at the end of the 21st century (approximately from 2070). Therefore, we hypothesize that the similar evolutions of phosphate concentration in HIS/A2 and of
405 incoming fluxes of phosphate through the Strait of Gibraltar throughout the simulation period are linked with changes in physical conditions. In this very dynamic part of the Mediterranean, changes in physical conditions linked with climate change are preconditioning the western basin to become more sensitive to nutrient fluxes thought the Strait of Gibraltar. A slight accumulation of about 0.015 mmol m^{-3} of phosphate is observed in the HIS/A2 simulation in the deep western basin. The signif-
410 icant difference between the HIS/A2 simulation and the control runs shows that the evolution of the Mediterranean physics linked with climate change is primarily responsible for the changes in phos-

phate concentration in the intermediate and deep western basin. Climate change effects lead to an accumulation of phosphate in the intermediate and deep layer that is probably linked to a decrease in surface primary productivity (hence, in nutrient consumption and export), decreased sediment fluxes (see Figure 6), and increased stratification, thus isolating most of the phosphate pool from the surface.

Nutrient concentrations in the eastern part of the basin are lower than in the western part (50 % lower phosphate concentration in the surface layer, about 30 % lower concentration in the intermediate layer and about 15 to 20 % lower concentration in the deep layer). In the surface layer, phosphate concentration decreases in the beginning of the simulation and remains low during the 21st century (from 0.022 mmol m^{-3} in 1980 to less that 0.015 mmol m^{-3} in 2000, Figure 7d). There is, however, a large annual variability in surface phosphate concentration with peaks up to 0.025 mmol m^{-3} in 2060. But the HIS/A2 simulation values are consistently below the CTRL concentrations showing an important effect of climate change on surface phosphate reduction. We observe in Figures 7e and 7f an accumulation of phosphate in the intermediate and deep layers (17 and 13 % respectively), with large decennial variability of phosphate concentration in the deep eastern basin. In both of these layers, HIS/A2 concentrations are higher than the CTRL concentrations.

The evolution of nitrate concentration shows an accumulation over the century in all regions of the intermediate and deep Mediterranean waters (between 9 and 20 %) in the HIS/A2 simulation (Figures 8b, 8c, 8e and 8f). In the surface western basin, the evolutions of the HIS/A2 and CTRL_RG simulations are similar, showing the regulating effects of fluxes through the Strait of Gibraltar (Figure 8d). In the intermediate layer, nitrate concentration in the HIS/A2 simulation is decreasing from 4.05 to 3.6 mmol m^{-3} between 1980 and 2030. After 2030, the concentration increases again up to 4.3 mmol m^{-3}. In the deep western basin, we observe a slight decrease in nitrate concentration in the controls from 4.4 to about 4.15 mmol m^{-3} whereas there is a slight accumulation from 4.5 to 4.75 mmol m^{-3} in the HIS/A2 over the simulation period.

In the eastern basin, the impacts of river discharges of nitrate seem to have large influence on the nitrate accumulation as shown by the similar evolution of HIS/A2 and CTRL_R simulations (Figures 8e and 8f). However, the evolution of physical conditions seems to have similarly large impacts on the nitrate concentrations in the eastern basin as shown by the difference between CTRL_R and HIS/A2 (see also Table 3). In particular, nitrate concentrations increase by about 0.5 mmol m^{-3} between 1980 and 2099 in the deep eastern basin. Approximately 50 % of this accumulation is due to river discharge. The large differences between the CTRL simulations and the HIS/A2 show that modification of circulation resulting from climate change have substantial impacts on the deep and intermediate nutrient concentrations. Figure 8d shows the contrasted effects of climate and biogeochemical changes. The strong difference between CTRL_R and CTRL concentrations at the beginning of the simulation (almost 0.4 mmol m^{-3}) indicates that riverine nutrient discharge has a strong influence on surface nitrate concentrations in the eastern basin and is responsible for an important

part of the eastern Mediterranean nitrate budget (see also Table 3). But the strong difference between
CTRL_R and HIS/A2 at the end of the century indicates that vertical stratification leads to a decrease
in surface layer nitrate concentrations, probably linked both with lower winter mixing and nutrient
consumption by phytoplankton.

3.4   Present and future surface nutrient concentrations, primary productivity and nutrient limitations in the surface Mediterranean

Figures 9 and 10 show the average surface concentrations of nitrate and phosphate in the beginning
of the century (1980–1999) and the relative concentration differences with the end of the century in
the HIS/A2 and CTRL simulations. In the Mediterranean Sea, primary productivity is mainly lim-
ited by these 2 nutrients and their evolution in the future may impact the productivity of the basin.
Figure 9 confirms the previous results showing an accumulation of nitrate in large zones of the basin,
except for the southwestern part of the western basin (Alboran Sea) and a small area in the south-
eastern Levantine.

On the contrary, Figure 10 shows that phosphate surface concentration is decreasing everywhere in
the basin except near the mouth of the Nile and in the Alboran Sea. The specific concentrations
observed next to the Nile mouth are linked with an inversion of the N:P ratio (i.e. increase in P
discharge and decrease in N discharge) in this river in our scenario. The distribution of surface phos-
phate concentration at the end of the century (2080–2099) shows that all P–rich areas of the eastern
basin at the beginning of our simulations are depleted by the end of the simulation. For instance, the
P rich areas around Crete and Cyprus are no longer observed in the 2080–2099 period (Figure 10).
Moreover, Figure 11 shows that these areas match productive zones. All the most productive zones of
the beginning of the century are reduced in size and intensity by the end of the century. The primary
production integrated over the euphotic layer (0–200 m) is reduced in our simulation by 10 % on
average between 1980–1999 and 2080–2099. However, Figure 11 shows a productivity decrease of
more than 50 % in areas such as the Aegean Sea and the Levantine Sea. In general, the differences in
surface biogeochemistry between the 1980–1999 and 2080–2099 periods are weaker in the western
basin because of the strong regulating impact of nutrient exchange through the Strait of Gibraltar.
The large scale reduction of surface primary productivity may be a cause for the observed reduction
in sedimentation (see Figure 6).

We also observe local changes in nutrient concentrations and primary production. For instance,
around Cyprus, changes in local concentrations of nutrients (decrease of about 50 % in phosphate
concentration) have substantial effects on primary productivity (decrease from 40-50 gC m^{-2} year^{-1}
to 20-30 gC m^{-2} year^{-1}). These mesoscale changes may be linked with local circulation changes

485 (such as mesoscale eddies). These observations show that the evolution of the Mediterranean bio-geochemistry is influenced by both meso and large scale circulations patterns.

Figure 12 presents the limiting nutrient calculated using PISCES half–saturation coefficients (see Aumont and Bopp, 2006). The limiting nutrient is derived from the minimal value of limitation fac-

490 tors. In the Monod–type model PISCES, nutrient–based growth rates follow a Michaëlis–Menten evolution with nutrient concentrations. In the present period, most of the productive areas are N and P colimited in the simulation (Figure 12). This includes regions such as the Gulf of Lions, the South Adriatic, the Aegean Sea and the northern Levantine. Future accumulation of nitrogen in the basin modifies the nutrient balance causing most eastern Mediterranean surface waters to become

495 P–limited. The total balance of phosphate is more negative in the future than in the present period whereas we observe an inverse situation for nitrate. Therefore, phosphate would become the major limiting nutrient in most of the regions where productivity is reduced such as the Aegean Sea, the northern Levantine basin and the South Adriatic.

500 ### 3.5   Modifications of the Mediterranean deep chlorophyll maximum

One specificity of Mediterranean biology is that most planktonic productivity occurs below the surface at a depth called the deep chlorophyll maximum (DCM). Hence, most of the chlorophyll concentration is not visible by satellites (Moutin et al., 2012). Figure 13 shows the average depth of the simulated DCM for the period 1980–1999 and for the period 2080–2099.

505

We observe that the DCM depth changes little during the simulation, even though the physical characteristics of the water masses do change (salinity and temperature). The DCM tends to deepen slightly in some regions such as the South Ionian and the Tyrrhenian basin. These results suggest that the DCM depth is not significantly altered in the future but the intensity of subsurface produc-

510 tivity seems reduced (see Figure 11).

Figure 14 shows the average vertical profiles of chlorophyll at the DYFAMED station (43.25° N, 7.52° E) and the average profiles for the western and eastern basins for the 1980–1999 and 2080–2099 periods. The results show that the subsurface chlorophyll maximum is still modeled at the end

515 of the century. At the DYFAMED station, the average DCM depth is unchanged but surface concentration is enhanced by about $25 \ 10^{-9}$ g L^{-1}. This shows that local variability in the Mediterranean circulation and biogeochemistry is important. However, we simulated seasonal variability in the chlorophyll concentration profiles at the station with intensity and depth of DCM reduced by about 40 % for some month (not shown). In the western basin, the subsurface maximum in the present and

520 future periods is located at the same depth (100–120 m), but the average chlorophyll concentration

is reduced by almost 50 %, which confirms the results from Figure 13. In the eastern basin, subsurface chlorophyll concentration is reduced and the subsurface chlorophyll maximum deepens from 100–120 m to below 150 m.

525 In the oligotrophic Mediterranean, the majority of the chlorophyll is produced within the DCM. The changes circulation combined with changes in fluxes through the Strait of Gibraltar and riverine inputs result in 17 % reduction in integrated chlorophyll production between the 1980–1999 and 2080–2099 periods. Table 4 reports total chlorophyll production in the 1980–1999, 2030–2049 and 2080–2099 periods of all the simulations in all Mediterranean subbasins (Figure 2 from Adloff et al.,

530 2015). Table 4 shows that chlorophyll production is stable over the CTRL simulation but decreases in all Mediterranean subbasins over the HIS/A2 simulation. The decrease in chlorophyll production is more important in the eastern regions, in particular in the Adriatic and Aegean Seas (-29 and -15 % respectively). In the western basin, the loss of chlorophyll is smaller (-13 %). The chlorophyll production is probably maintained by the enhancement of nutrient fluxes through the Strait of

535 Gibraltar (chlorophyll production in CTRL_RG does not significantly decrease in the western basin).

The results indicate that 85 % of the reduction in chlorophyll production in the future period modeled in the HIS/A2 simulation is explained by climate effects (difference between HIS/A2 and CTRL_RG). However, the effects of increased nutrient inputs through the Strait of Gibraltar, de-

540 creased riverine phosphate inputs and increased riverine inputs of nitrate seem to have opposing effects to climate and circulation changes on chlorophyll production. In particular, in the western basin, changes in riverine discharge of nutrients seem to reduce chlorophyll production (see CTRL_R values), whereas changes in fluxes through the Strait of Gibraltar seem to enhance chlorophyll production (see CTRL_RG).

545 **3.6 Plankton biomass evolution**

Most of the biological activity in the marine environment is confined to the euphotic layer which is confined to the upper 200 m. Figure 15 shows the evolution of nanophytoplankton and diatom concentrations in the top 200 m for the entire simulation period in all simulations in the western and eastern basins. In HIS/A2, we observe lower biomass for both phytoplankton classes across

550 the Mediterranean Sea at the end of the century than at the beginning. In general, diatoms seem more sensitive to climate change and their biomass decreases more sharply than nanophytoplankton. Moreover, Figure 15c shows that diatom concentrations in the western basin seem to be sensitive to changes in nutrient input across the Strait of Gibraltar as indicated by the large difference between CTRL_RG and CTRL_R. However, the low diatom concentration observed in HIS/A2 indicates that

555 the evolution of the diatom concentration over the 21st century is primarily influenced by climatic drivers.

Figure 16 shows the evolution of zooplankton biomass in the top 200 m during the simulation. The same general evolution is found than for the simulated phytoplankton: a decrease in microzoo-plankton during 1980–2000 (from 0.165 to approximately 0.114 mmol m^{-3}), after which it remains stable and consistently below the CTRL values until the end of the simulation in 2100 in all basins. A large drawdown in mesozooplankton levels is simulated in the eastern basin. The average meso-zooplankton concentration in the eastern part of the Mediterranean declines by almost 60 % in 2099 in comparison to 1980. However, the average mesozooplankton concentration over the 2080–2099 period is only slightly lower than the average concentration over the 1980–1999 period (0.10 and 0.11 mmol m^{-3} respectively) because the decline in concentration occurs within the first years of the HIS/A2 simulation. In the western basin, we observe a marked decrease of mesozooplankton concentrations between 1980 and 2040 (a decrease of 0.05 mmol m^{-3} is observed between these 2 periods). After 2040, mesozooplankton surface concentration increases regularly to similar values than at the beginning of the simulation. This evolution is similar to those of nutrient concentrations in surface waters of the western basin (Figure 7). In the PISCES model, zooplankton, and in partic-ular mesozooplankton is highly sensitive to the variations of external climatic and biogeochemical conditions because that is the highest trophic level represented. Owing to their bottom–up control, zooplankton canalize all changes at the basin scale and ultimately displays the largest response. This behavior is similar to the trophic amplification observed by Chust et al. (2014) and Lefort et al. (2015).

Altogether, the analysis of plankton biomass evolution during the simulation period suggests that primary and secondary production in the eastern basin are more sensitive to climate change than the western basin in this simulation. The eastern part of the basin is more isolated from the open Atlantic Ocean than is the western part and it receives less nutrients from the Atlantic and from coastal inputs. The eastern basin is also deeper and less productive than the western basin (Crispi et al., 2001). The eastern basin exhibits a decline in the phytoplankton biomass that is similar to the decline in the phosphate concentration. Biological production is mainly P–limited in this basin (see also Figure 12). Therefore, the constant low concentrations of phosphate observed throughout this century limit biological production and keep plankton biomass at low levels.

4 Discussion

4.1 Biogeochemical forcings

Climate change may impact all drivers of biogeochemical cycles in the ocean. In the case of semi–enclosed seas like the Mediterranean, the biogeochemistry is primarily influenced by external sources of nutrients (namely rivers, Atlantic and atmospheric inputs, see Ludwig et al., 2009; Krom et al.,

2010) and modification of the physical ocean (vertical mixing, horizontal advection, ..., see San-tinelli et al., 2012). Nutrient fluxes from external sources (rivers, aerosols and fluxes through the Strait of Gibraltar) may evolve separately and differently depending on socio-economic decisions and climate feedbacks. In this study, different scenarios were used for river inputs ("Order from Strength" from Ludwig et al., 2010, based on the Millenium Ecosystem Assessment report) and for Atlantic nutrient concentrations (SRES/A2 from Dufresne et al., 2013). Scenarios from the MEA report are based on different assumptions from the IPCC SRES scenarios used to compute freshwater runoff in the HIS/A2 simulation. Moreover, the Ludwig et al. (2010) nutrient discharge transient scenario does not represent the interannual variability of nutrient runoff from rivers. Other studies by Herrmann et al. (2014) and Macias et al. (2015) used continued present–day discharge of nutrients. As there is no consensus nor validated scenario for nutrient fluxes from riverine runoff in the Mediterranean, we chose to use one scenario from Ludwig et al. (2010). This scenario has the advantage of being derived from a coherent modeling framework. However, according to these authors, the socio–economic decisions made in the 21st century will influence nitrate and phosphate discharge over the Mediterranean. It is difficult to forecast these decisions and the resulting changes in nutrient fluxes are uncertain. Moreover, our results emphasize that the biogeochemistry in many coastal regions of the Mediterranean Sea such as the Adriatic Sea are highly influenced by riverine nutrient inputs, which is in accordance with previous work (e.g. Spillman et al., 2007, and references therein). In these regions, the effects of nutrient runoff from rivers seem more important than climate change effects (see Table 4). In the Adriatic basin, table 3 shows that riverine nitrate discharge is responsible for 41 % increase in nitrate concentration over the simulation period (difference between the 1980–1999 and the 2080–2099 periods). In the CTRL_RG simulation, nitrate concentrations are similar to the CTRL_R simulation showing no influence of fluxes through the Strait of Gibraltar in this region. Finally, nitrate concentrations in the HIS/A2 simulation are close to the CTRL_R values showing that most of the nitrate evolution in this region is linked with riverine discharge. Therefore, the choice of river runoff scenario will greatly influence the results in these regions. Associated discrepancies and the uncertainties linked with the use of inconsistent scenarios in our simulation should be addressed by developing a more integrated modelling framework to study the impacts of climate change on the Mediterranean Sea biogeochemistry.

No transient atmospheric deposition was considered in this study because there is, to our knowledge, no transient scenario for atmospheric deposition evolution over the Mediterranean Sea. However, in order to evaluate the potential effects of aerosol deposition on the future Mediterranean Sea, we performed 2 simulations with respectively total nitrogen ($NH_4 + NO_3$) deposition (labeled HIS/A2_N) and total nitrogen and natural dust deposition (labeled HIS/A2_NALADIN). The deposition fields are derived from the global model LMDz–INCA and the regional model ALADIN–Climat respectively (see Richon et al., 2017, and references therein for description and evaluation of the atmospheric models). The atmospheric deposition fields represent present–day aerosol deposition fluxes

18

(1997–2012 and 1980–2012 for total nitrogen and dust deposition respectively) that are repeated over the 1980–2099 simulation period. The following figure (Figure 17) shows the relative effects of total nitrogen and natural dust deposition on surface primary production in the 1980–1999 and 2080–2099 periods. As shown in Richon et al. (2017), dust deposition is a source of phosphate for the surface Mediterranean. As our HIS/A2 simulation shows a decrease in surface PO_4 concentrations, thus accentuating phosphate limitation over the Mediterranean basin by the end of the 21st century, the relative effects of phosphate deposition from dust are increased in the 2080–2099 period in comparison to the 1980–1999 period. Conversely, nitrogen atmospheric deposition has very little effect on Mediterranean primary production at the end of the simulation period because most of the basin is not N–limited.

4.2 Climate change scenario

Although the physical model adequately represents the MHTC (Adloff et al., 2015), there are many uncertainties linked with climate change projections. Some are discussed in Somot et al. (2006), in particular, the need to using different IPCC scenarios for climate change projections and MTHC changes. Adloff et al. (2015) apply an ensemble of SRES scenarios and boundary conditions to the Mediterranean Sea and discuss their effects on MTHC. In particular, their results suggests that the choice of atmospheric and Atlantic conditions has a strong influence on the MTHC. The A2 scenario that we used was the only available with 3–D daily forcings for coupling with the PISCES biogeochemical model. However, Adloff et al. (2015) showed that other SRES scenarios such as the A1B or B1 may lead to a future decrease in the vertical stratification with probably different consequences on the Mediterranean Sea biogeochemistry. Our study should be considered as a first step for transient modeling of the Mediterranean Sea biogeochemistry but should be complemented by new simulations that explore the various sources of uncertainty (model choice, internal variability, scenario choice) once appropriate forcings become available for multiple models as expected from the Med–CORDEX initiative (Ruti et al., 2016).

4.3 Uncertainties from the PISCES model

The evaluation of the CTRL simulation showed that NEMOMED8/PISCES is stable over time in spite of a slight drift in nitrate concentrations (see Figure 8). Nutrient concentrations in the intermediate and deep layers were shown to be underestimated in comparison to measurements (see appendix). Nutrient concentrations can be underestimated by up to 50 %, in particular in the deep eastern basin. Moreover, nitrate fluxes from coastal discharge in CTRL are lower than in HIS/A2. The low riverine discharge and the imbalance in sources and sinks explains the loss of nitrate in the CTRL (see Figures 8 and 9). Organic forms of nutrients are not directly available to phytoplankton in this version of PISCES, and are not included in our nutrient budgets. Powley et al. (2017) show that

19

organic forms of nutrient are an important part of the Mediterranean elemental budgets. Therefore,
665   we may be missing a part of the N and P budgets in our calculations. The simulated chlorophyll–a
vertical profiles at the DYFAMED station show a correct representation of the subsurface productiv-
ity maximum of the Mediterranean in spite of a mismatch in the subsurface chlorophyll maximum
depth between model and measurements. Model values were not corrected to match data, and we
are therefore conscious that the uncertainties in the representation of present–day biogeochemistry
670   by the PISCES model may be propagated in the future.

In the PISCES version used in this study, nitrate and phosphate concentration variations are linked
by the Redfield ratio (Redfield et al., 1963). The Redfield hypothesis of a fixed nutrient ratio used
for plankton growth and excretion holds true for most parts of the global ocean, but may not be true
for oligotrophic regions such as the Mediterranean Sea (e.g. Béthoux and Copin-Montégut, 1986).
675   Moreover, changes in nutrient balance influence the nutrient limitations as shown by Figure 12. The
results simulated with the Redfieldian hypothesis are coherent with the observed variations of nutri-
ent supply to the Mediterranean Sea and yield realistic biological productivity. But results concerning
nutrient limitations might change in a non Redfieldian biogeochemistry model.

4.4   Climate versus biogeochemical changes effects

680   Figure 18 summarizes the fluxes of phosphate and nitrate in and out of the Mediterranean considered
in this study.

In general, the sum of nitrogen net fluxes into the Mediterranean basin (Riverine, Gibraltar Strait
and sedimentary sources and sinks) increases by 39 % at the end of the century in the scenario
685   (HIS/A2) whereas it is increased by 23 % in the control (CTRL) in comparison to the beginning of
the simulation (1980). The balance between inputs and outputs of phosphorus increases by 9 % in
the scenario and by 11 % in the control (net gain of phosphorus in the basin). These results suggest
a significant accumulation of nitrogen in the Mediterranean basin over the century when phosphorus
fluxes can be considered roughly stable. The strong decrease in sedimentation (Figure 6) occurring
690   in spite of an enhancement in nutrient flux, coming from the Atlantic and an enhanced nitrate river
flux may be linked to the decrease in vertical water fluxes. This would explain the accumulation
of phosphate and nitrate in the deep layers of the Mediterranean Sea (Figures 7c, 7f,8c and 8f).
The difference between HIS/A2 and CTRL_RG phosphate concentrations (Figure 7) indicates that
the variations of phosphate concentrations during the 21st century are primarily linked with climate
695   change whereas nitrate concentration seems equally sensitive to changes in biogeochemical forcings.
To our knowledge, this is the first attempt to study the basin–scale biogeochemical evolution using
a transient business–as–usual (A2) climate change scenario. Lazzari et al. (2014) tested the effects
of several land–use change scenarios on the A1B SRES climate change scenario over 10–years time
slices. They found a general decrease in phytoplankton and zooplankton biomasses (about 5 %)

700   that is lower than in our severe climate change scenario. In our simulations, average phytoplankton
      biomass decreases by about 2 to 30 % (see Figure 15 and average zooplankton biomass decreases
      by about 8 and 12 % (see Figure 16. However, our transient simulations revealed non linear trends
      in plankton biomass evolution. Lazzari et al. (2014) also conclude that the river mouth regions are
      highly sensitive because the Mediterranean Sea is influenced by external nutrient inputs. Our results
705   show the same sensitivity of the Mediterranean to external nutrient inputs. Herrmann et al. (2014)
      studied the transient biogeochemical evolution of the northwestern Mediterranean Sea under the A2
      and A1B scenarios with the coupled ECO3M–S/SYMPHONIE model. But they used present–day
      conditions for biogeochemical forcings, as did Macias et al. (2015). Results from Herrmann et al.
      (2014) indicate that chlorophyll concentration and plankton biomass in the northwestern Mediter-
710   ranean increase slightly as a result of vertical stratification. Our results indicate that the contrasting
      effects of vertical stratification biogeochemical changes may lead to a decrease in chlorophyll con-
      centration, phytoplankton and zooplankton biomass content of up to 50 % locally and between 2
      and 30 % at the basin scale as indicated by Figures 14, 15 and 16. The modifications of chloro-
      phyll production and plankton biomass are linked to changes in nutrient limitation (Figure 12). Our
715   finding that most of the Mediterranean basin is N and P co–limited seems in contrast with previous
      literature on the matter (see Krom et al., 2004, 2010; Pujo-Pay et al., 2011, and references therein).
      These authors found from analyses of the N:P ratio of the waters a clear phosphorus limitation in the
      major part of the Mediterranean. The discrepancy between our results and literature estimates comes
      from the way we calculate nutrient limitations. Considering how low nutrient concentrations are
720   in the Mediterranean and how low the nutrient limitation factors are, the small difference between
      the limitation factors indicate that the Mediterranean is both limited in P and N. Finding no clear
      definition of nutrient co–limitation, we propose to consider that N and P are co-limiting when the
      difference in limitation factors is less than 1 %. This definition of nutrient co–limitation applies well
      to the Mediterranean case because of the very low nutrient concentrations. Chust et al. (2014) have
725   shown that regional seas and in particular the Aegean and Adriatic were sensitive to trophic ampli-
      fication. Our results seem to agree with these conclusions by showing sign of trophic amplification
      (see Figures 15 and 16). Finally, Luna et al. (2012) hypothesise that the warm temperature of the
      deep Mediterranean may be a cause for important nutrient recycling via prokaryotic metabolism. In
      the version of PISCES used in this study, nutrient recycling is dependant on oxygen, depth, plankton
730   biomass and bacterial activity. Therefore, we could not observe the effects of temperature on nutrient
      recycling.

      Results from our different control simulations indicates the extent to which the choice of the biogeo-
      chemical forcing scenario may influence the future evolution of the Mediterranean Sea biogeochem-
      istry. In particular, nutrient inputs through the Strait of Gibraltar have substantial consequences on
735   the western basin. Results from Figures 7a and 8a and Table 4 indicate that the increase in nutrient
      inputs through the Strait of Gibraltar at the end of the century is responsible for a 2.5 % increase in

chlorophyll concentration in the western basin during the 2080–2099 period. Moreover, climate and nutrient forcing changes may have contrasting influences on the Mediterranean Sea biogeochemistry. Stratification may lead to increased productivity in the surface because of the nutrient concentration

740 increase (see also Macias et al., 2015), while decreasing coastal discharges of phosphate may decrease the productivity in the basin.

Conclusion

This study aims at assessing the transient effects of climate and biogeochemical changes on the Mediterranean Sea biogeogeochemistry under the high–emission IPCC A2 scenario. The NEMOMED8/PISCES

745 model adequately reproduces the main characteristics of the Mediterranean Sea: the west–to–east gradient of productivity, the main productive zones and the presence of a DCM. Hence, it appears reasonable to use it to study the future evolution of the biogeochemistry of the Mediterranean basin in response to increasing atmospheric CO_2 and resulting climate change. For the first time, we performed a continuous simulation over the entire period of the future IPCC scenario (A2), between

750 1980 and 2099.

This study illustrates how future changes in physical and biogeochemical conditions, including warming, increased stratification, and changes in Atlantic and river inputs, can lead to a significant accumulation of nitrate and a decrease in biological productivity in the surface, thus affecting the entire Mediterranean ecosystem.

755 Our results also illustrate how climate change and nutrient inputs from riverine sources and fluxes through the Strait of Gibraltar have contrasted influences on the Mediterranean Sea productivity. In particular, the biogeochemistry in the western basin displays similar nutrient trends as does its input across the Strait of Gibraltar. Therefore, it appears critical to correctly represent the future variations of external biogeochemical forcings of the Mediterranean Sea as they may have equally important

760 influence on biogeochemical cycles as climate. The biogeochemistry of the eastern basin is more sensitive to vertical mixing and river inputs than the western basin (that receives regulating effects from exchanges through the Strait of Gibraltar) and the stratification observed in the future leads to a reduction in surface productivity.

Finally, this study accounts for the changes in fluxes through the Strait of Gibraltar and riverine

765 inputs, but some potentially important sources are missing such as direct wastewater discharge, submarine groundwater and atmospheric deposition. Measurements and models are still missing in order to include comprehensive datasets for past and future evolution of these nutrient sources. The HIS/A2_N and HIS/A2_NALADIN simulations presented in the discussion section include continued present–day nitrogen and phosphate deposition. Although these atmospheric fluxes have been

770 evaluated previously and were shown to represent correctly the deposition fluxes, there is no guarantee that these fluxes are going to remain constant over the next century. Results showed that the

22

future sensitivity of the Mediterranean to atmospheric deposition depends on the surface nutrient limitations. However, there is to our knowledge no available transient scenario for the 21st century evolution of atmospheric deposition and no ensemble simulations to assess the future evolution of the

775 Mediterranean Sea under different climate change scenarios. A new generation of fully coupled regional models have been developed and used to study aerosols climatic impacts (Nabat et al., 2015). These models include a representation of the ocean, atmosphere, aerosols and rivers and should be used to perform consistent future climate projections at the Mediterranean regional scale.

Appendix A: Evaluation of the NEMOMED8/PISCES model

785 The comparison of modeled surface chlorophyll–*a* concentration with satellite estimates has revealed that the model correctly simulates the main characteristics observed in the Mediterranean Sea (Figures 1 and 2). Comparison with in situ observation provides more refined estimates.

Figure A1 presents the average chlorophyll–a profiles at the DYFAMED station (43.25°N, 7.52°E)

790 compared with measured concentrations for the month of February (low stratification, high productivity) and May (end of spring bloom, beginning of stratification and DCM appearance). There are few data points below 200 m. The model produces the characteristic of the deep chlorophyll maximum generated in May, even if its depth is too important. The colors show that the model represents some interannual variability in chlorophyll production in spite of the consistent bias.

795

The overestimation of the DCM depth may be due to the overestimation of nitracline and phosphacline as shown by figure A2. This Figure shows the vertical profiles of nitrate and phosphate at the DYFAMED station in May, colors represent the different years in the model and in the observation.

800

The vertical distribution of nitrate and phosphate concentrations along a West–to–East transect is shown in Figure A3. The model produces the salient West–to–East gradient of nutrient concentrations. Concentrations in the surface layer seem correct. The nutricline is located 100 to 150 m deep in the western basin and deepens around 180 to 200 m in the eastern basin. Although the model

805 represents the spatial variability of the nutricline, it is too smooth, leading to the underestimation of

23

deep water concentrations (by about 30 to 50 %).

References

Adloff, F., Somot, S., Sevault, F., Jordà, G., Aznar, R., Déqué, M., Herrmann, M., Marcos, M., Dubois, C.,
Padorno, E., Alvarez-Fanjul, E., and Gomis, D.: Mediterranean Sea response to climate change in an ensem-
ble of twenty first century scenarios, Climate Dynamics, 45, 2775–2802, doi:10.1007/s00382-015-2507-3,
http://link.springer.com/article/10.1007/s00382-015-2507-3, 2015.

Albouy, C., Leprieur, F., Le Loc'h, F., Mouquet, N., Meynard, C. N., Douzery, E. J. P., and Mouillot, D.:
Projected impacts of climate warming on the functional and phylogenetic components of coastal Mediter-
ranean fish biodiversity, Ecography, 38, 681–689, doi:10.1111/ecog.01254, http://doi.wiley.com/10.1111/
ecog.01254, 2015.

Andrello, M., Mouillot, D., Somot, S., Thuiller, W., and Manel, S.: Additive effects of climate change on
connectivity between marine protected areas and larval supply to fished areas, Diversity and Distributions,
21, 139–150, doi:10.1111/ddi.12250, http://onlinelibrary.wiley.com/doi/10.1111/ddi.12250/abstract, 2015.

Auger, P. A., Ulses, C., Estournel, C., Stemmann, L., Somot, S., and Diaz, F.: Interannual control of plankton
communities by deep winter mixing and prey/predator interactions in the NW Mediterranean: Results from
a 30-year 3D modeling study, Progress in Oceanography, 124, 12–27, doi:10.1016/j.pocean.2014.04.004,
http://www.sciencedirect.com/science/article/pii/S0079661114000524, 2014.

Aumont, O. and Bopp, L.: Globalizing results from ocean in situ iron fertilization studies: GLOBALIZING
IRON FERTILIZATION, Global Biogeochemical Cycles, 20, n/a–n/a, doi:10.1029/2005GB002591, http:
//doi.wiley.com/10.1029/2005GB002591, 2006.

Beuvier, J., Sevault, F., Herrmann, M., Kontoyiannis, H., Ludwig, W., Rixen, M., Stanev, E., Béranger,
K., and Somot, S.: Modeling the Mediterranean Sea interannual variability during 1961–2000: Fo-
cus on the Eastern Mediterranean Transient, Journal of Geophysical Research: Oceans, 115, C08 017,
doi:10.1029/2009JC005950, http://onlinelibrary.wiley.com/doi/10.1029/2009JC005950/abstract, 2010.

Bonnet, S., Grosso, O., and Moutin, T.: Planktonic dinitrogen fixation along a longitudinal gradient across
the Mediterranean Sea during the stratified period (BOUM cruise), Biogeosciences, 8, 2257–2267,
doi:10.5194/bg-8-2257-2011, http://www.biogeosciences.net/8/2257/2011/, 2011.

Bosc, E., Bricaud, A., and Antoine, D.: Seasonal and interannual variability in algal biomass and
primary production in the Mediterranean Sea, as derived from 4 years of SeaWiFS observations:
MEDITERRANEAN SEA BIOMASS AND PRODUCTION, Global Biogeochemical Cycles, 18, n/a–n/a,
doi:10.1029/2003GB002034, http://doi.wiley.com/10.1029/2003GB002034, 2004.

Béthoux, J. P. and Copin-Montégut, G.: Biological fixation of atmospheric nitrogen in the Mediterranean Sea,
Limnology and Oceanography, 31, 1353–1358, doi:10.4319/lo.1986.31.6.1353, http://onlinelibrary.wiley.
com/doi/10.4319/lo.1986.31.6.1353/abstract, 1986.

Béthoux, J. P., Morin, P., Chaumery, C., Connan, O., Gentili, B., and Ruiz-Pino, D.: Nutrients in the Mediter-
ranean Sea, mass balance and statistical analysis of concentrations with respect to environmental change, Ma-
rine Chemistry, 63, 155–169, doi:10.1016/S0304-4203(98)00059-0, http://www.sciencedirect.com/science/
article/pii/S0304420398000590, 1998.

Christodoulaki, S., Petihakis, G., Kanakidou, M., Mihalopoulos, N., Tsiaras, K., and Triantafyllou, G.: Atmo-
spheric deposition in the Eastern Mediterranean. A driving force for ecosystem dynamics, Journal of Ma-

rine Systems, 109-110, 78–93, doi:10.1016/j.jmarsys.2012.07.007, http://linkinghub.elsevier.com/retrieve/
pii/S0924796312001583, 2013.

Chust, G., Allen, J. I., Bopp, L., Schrum, C., Holt, J., Tsiaras, K., Zavatarelli, M., Chifflet, M., Cannaby, H.,
850   Dadou, I., Daewel, U., Wakelin, S. L., Machu, E., Pushpadas, D., Butenschon, M., Artioli, Y., Petihakis,
G., Smith, C., Garçon, V., Goubanova, K., Vu, B. L., Fach, B. A., Salihoglu, B., Clementi, E., and Irigoien,
X.: Biomass changes and trophic amplification of plankton in a warmer ocean, Global Change Biology, 20,
2124–2139, doi:10.1111/gcb.12562, https://onlinelibrary.wiley.com/doi/abs/10.1111/gcb.12562, 2014.

Civitarese, G., Gacic, M., Lipizer, M., and Borzelli, G. L. E.: On the impact of the Bimodal Oscillating Sys-
855   tem (BiOS) on the biogeochemistry and biology of the Adriatic and Ionian Seas (Eastern Mediterranean),
Biogeosciences, 7, 3987–3997, doi:10.5194/bg-7-3987-2010, wOS:000285574100006, 2010.

Claustre, H., Morel, A., Hooker, S. B., Babin, M., Antoine, D., Oubelkheir, K., Bricaud, A., Leblanc, K.,
Quéguiner, B., and Maritorena, S.: Is desert dust making oligotrophic waters greener?, Geophysical Research
Letters, 29, 107–1–107–4, doi:10.1029/2001GL014056, https://agupubs.onlinelibrary.wiley.com/doi/abs/10.
860   1029/2001GL014056, 2002.

Cork, S., Peterson, G., Petschel-Held, G., Alcamo, J., Alder, J., Bennett, E., Carr, E., Deane, D., Nel-
son, G., Ribeiro, T., and others: Four scenarios, Ecosystems and human well-being: Scenarios, 2, http:
//www.academia.edu/download/31005604/Millennium_assessment.pdf, 2005.

Crispi, G., Mosetti, R., Solidoro, C., and Crise, A.: Nutrients cycling in Mediterranean basins: the role
865   of the biological pump in the trophic regime, Ecological Modelling, 138, 101–114, doi:10.1016/S0304-
3800(00)00396-3, http://www.sciencedirect.com/science/article/pii/S0304380000003963, 2001.

d'Ortenzio, F. and Ribera d'Alcalà, M.: On the trophic regimes of the Mediterranean Sea: a satellite analysis,
Biogeosciences, 6, 139–148, http://www.biogeosciences.net/6/139/2009/bg-6-139-2009.html, 2009.

Déqué, M., Dreveton, C., Braun, A., and Cariolle, D.: The ARPEGE/IFS atmosphere model: a contribution
870   to the French community climate modelling, Climate dynamics, 10, 249–266, http://cat.inist.fr/?aModele=
afficheN&cpsidt=4250659, 1994.

Dubois, C., Somot, S., Calmanti, S., Carillo, A., Déqué, M., Dell'Aquilla, A., Elizalde, A., Gualdi, S., Jacob,
D., L'Hévéder, B., Li, L., Oddo, P., Sannino, G., Scoccimarro, E., and Sevault, F.: Future projections of
the surface heat and water budgets of the Mediterranean Sea in an ensemble of coupled atmosphere-ocean
875   regional climate models, Climate Dynamics, 39, 1859–1884, doi:10.1007/s00382-011-1261-4, http://adsabs.
harvard.edu/abs/2012ClDy...39.1859D, 2012.

Dufresne, J.-L., Foujols, M.-A., Denvil, S., Caubel, A., Marti, O., Aumont, O., Balkanski, Y., Bekki, S., Bel-
lenger, H., Benshila, R., Bony, S., Bopp, L., Braconnot, P., Brockmann, P., Cadule, P., Cheruy, F., Codron, F.,
Cozic, A., Cugnet, D., Noblet, N. d., Duvel, J.-P., Ethé, C., Fairhead, L., Fichefet, T., Flavoni, S., Friedling-
880   stein, P., Grandpeix, J.-Y., Guez, L., Guilyardi, E., Hauglustaine, D., Hourdin, F., Idelkadi, A., Ghattas,
J., Joussaume, S., Kageyama, M., Krinner, G., Labetoulle, S., Lahellec, A., Lefebvre, M.-P., Lefevre, F.,
Levy, C., Li, Z. X., Lloyd, J., Lott, F., Madec, G., Mancip, M., Marchand, M., Masson, S., Meurdesoif, Y.,
Mignot, J., Musat, I., Parouty, S., Polcher, J., Rio, C., Schulz, M., Swingedouw, D., Szopa, S., Talandier,
C., Terray, P., Viovy, N., and Vuichard, N.: Climate change projections using the IPSL-CM5 Earth Sys-
885   tem Model: from CMIP3 to CMIP5, Climate Dynamics, 40, 2123–2165, doi:10.1007/s00382-012-1636-1,
https://link.springer.com/article/10.1007/s00382-012-1636-1, 2013.

Dulac, F., BUAT-MÉNARD, P., Ezat, U., Melki, S., and Bergametti, G.: Atmospheric input of trace metals to the western Mediterranean: uncertainties in modelling dry deposition from cascade impactor data, Tellus B, 41, 362–378, http://onlinelibrary.wiley.com/doi/10.1111/j.1600-0889.1989.tb00315.x/full, 1989.

890 Dunić, N., Vilibić, I., Šepić, J., Somot, S., and Sevault, F.: Dense water formation and BiOS-induced variability in the Adriatic Sea simulated using an ocean regional circulation model, Climate Dynamics, doi:10.1007/s00382-016-3310-5, http://link.springer.com/10.1007/s00382-016-3310-5, 2016.

Faugeras, B., Lévy, M., Mémery, L., Verron, J., Blum, J., and Charpentier, I.: Can biogeochemical fluxes be recovered from nitrate and chlorophyll data? A case study assimilating data in the Northwestern Mediterranean

895 Sea at the JGOFS-DYFAMED station, Journal of Marine Systems, 40-41, 99–125, doi:10.1016/S0924-7963(03)00015-0, http://www.sciencedirect.com/science/article/pii/S0924796303000150, 2003.

Fichaut, M., Garcia, M. J., Giorgetti, A., Iona, A., Kuznetsov, A., Rixen, M., and Group, M.: MEDAR/MEDATLAS 2002: A Mediterranean and Black Sea database for operational oceanography, in: Elsevier Oceanography Series, edited by H. Dahlin, K. Nittis and S. E. Petersson, N. C. F., vol. 69 of *Building*

900 *the European Capacity in Operational OceanographyProceedings of the Third International Conference on EuroGOOS*, pp. 645–648, Elsevier, http://www.sciencedirect.com/science/article/pii/S0422989403801071, 2003.

Gallisai, R., Peters, F., Volpe, G., Basart, S., and Baldasano, J. M.: Saharan Dust Deposition May Affect Phytoplankton Growth in the Mediterranean Sea at Ecological Time Scales, PLoS ONE, 9, e110 762,

905 doi:10.1371/journal.pone.0110762, http://dx.plos.org/10.1371/journal.pone.0110762, 2014.

Gibelin, A.-L. and Déqué, M.: Anthropogenic climate change over the Mediterranean region simulated by a global variable resolution model, Climate Dynamics, 20, 327–339, doi:10.1007/s00382-002-0277-1, https://link.springer.com/article/10.1007/s00382-002-0277-1, 2003.

Giorgi, F.: Climate change hot-spots, Geophysical Research Letters, 33, L08 707, doi:10.1029/2006GL025734,

910 http://onlinelibrary.wiley.com/doi/10.1029/2006GL025734/abstract, 2006.

Giorgi, F. and Lionello, P.: Climate change projections for the Mediterranean region, Global and Planetary Change, 63, 90–104, doi:10.1016/j.gloplacha.2007.09.005, http://www.sciencedirect.com/science/article/pii/S0921818107001750, 2008.

Gómez, F.: The role of the exchanges through the Strait of Gibraltar on the budget of elements in

915 the Western Mediterranean Sea: consequences of human-induced modifications, Marine Pollution Bulletin, 46, 685–694, doi:10.1016/S0025-326X(03)00123-1, http://www.sciencedirect.com/science/article/pii/S0025326X03001231, 2003.

Guieu, C., Ridame, C., Pulido-Villena, E., Bressac, M., Desboeufs, K., and Dulac, F.: Dust deposition in an oligotrophic marine environment: impact on the carbon budget, Biogeosciences Discussions, 11, 1707–1738,

920 doi:10.5194/bgd-11-1707-2014, http://www.biogeosciences-discuss.net/11/1707/2014/, 2014.

Harley, C. D. G., Randall Hughes, A., Hultgren, K. M., Miner, B. G., Sorte, C. J. B., Thornber, C. S., Rodriguez, L. F., Tomanek, L., and Williams, S. L.: The impacts of climate change in coastal marine systems, Ecology Letters, 9, 228–241, doi:10.1111/j.1461-0248.2005.00871.x, http://onlinelibrary.wiley.com/doi/10.1111/j.1461-0248.2005.00871.x/abstract, 2006.

925 Hattab, T., Albouy, C., Lasram, F. B. R., Somot, S., Le Loc'h, F., and Leprieur, F.: Towards a better understanding of potential impacts of climate change on marine species distribution: a multiscale modelling approach,

Global Ecology and Biogeography, 23, 1417–1429, doi:10.1111/geb.12217, http://onlinelibrary.wiley.com/doi/10.1111/geb.12217/abstract, 2014.

Herrmann, M., Sevault, F., Beuvier, J., and Somot, S.: What induced the exceptional 2005 convection event in the northwestern Mediterranean basin? Answers from a modeling study, Journal of Geophysical Research: Oceans, 115, C12 051, doi:10.1029/2010JC006162, http://onlinelibrary.wiley.com/doi/10.1029/2010JC006162/abstract, 2010.

Herrmann, M., Diaz, F., Estournel, C., Marsaleix, P., and Ulses, C.: Impact of atmospheric and oceanic interannual variability on the Northwestern Mediterranean Sea pelagic planktonic ecosystem and associated carbon cycle, Journal of Geophysical Research: Oceans, 118, 5792–5813, doi:10.1002/jgrc.20405, http://onlinelibrary.wiley.com/doi/10.1002/jgrc.20405/abstract, 2013.

Herrmann, M., Estournel, C., Adloff, F., and Diaz, F.: Impact of climate change on the northwestern Mediterranean Sea pelagic planktonic ecosystem and associated carbon cycle, Journal of Geophysical Research: Oceans, 119, 5815–5836, doi:10.1002/2014JC010016, http://onlinelibrary.wiley.com/doi/10.1002/2014JC010016/abstract, 2014.

Huertas, I. E., Ríos, A. F., García-Lafuente, J., Navarro, G., Makaoui, A., Sánchez-Román, A., Rodriguez-Galvez, S., Orbi, A., Ruíz, J., and Pérez, F. F.: Atlantic forcing of the Mediterranean oligotrophy, Global Biogeochemical Cycles, 26, GB2022, doi:10.1029/2011GB004167, http://onlinelibrary.wiley.com/doi/10.1029/2011GB004167/abstract, 2012.

Ibello, V., Cantoni, C., Cozzi, S., and Civitarese, G.: First basin-wide experimental results on N2 fixation in the open Mediterranean Sea, Geophysical Research Letters, 37, L03 608, doi:10.1029/2009GL041635, http://onlinelibrary.wiley.com/doi/10.1029/2009GL041635/abstract, 2010.

IPCC: Managing the Risks of Extreme Events and Disasters to Advance Climate Change Adaptation. A Special Report of Working Groups I and II of the Intergovernmental Panel on Climate Change, Cambridge University Press, Cambridge, United Kingdom, and New York, NY, USA, 2012.

IPCC and Working Group III: Emissions scenarios. a special report of IPCC Working Group III, Intergovernmental Panel on Climate Change, Geneva, http://catalog.hathitrust.org/api/volumes/oclc/59436339.html, oCLC: 891560334, 2000.

Jordà, G., Marbà, N., and Duarte, C. M.: Mediterranean seagrass vulnerable to regional climate warming, Nature Climate Change, 2, 821–824, doi:10.1038/nclimate1533, http://www.nature.com/nclimate/journal/v2/n11/abs/nclimate1533.html?foxtrotcallback=true, 2012.

Klein, B., Roether, W., Kress, N., Manca, B. B., Ribera d'Alcala, M., Souvermezoglou, E., Theocharis, A., Civitarese, G., and Luchetta, A.: Accelerated oxygen consumption in eastern Mediterranean deep waters following the recent changes in thermohaline circulation, Journal of Geophysical Research: Oceans, 108, 8107, doi:10.1029/2002JC001454, http://onlinelibrary.wiley.com/doi/10.1029/2002JC001454/abstract, 2003.

Krom, M. D., Herut, B., and Mantoura, R. F. C.: Nutrient budget for the Eastern Mediterranean: Implications for phosphorus limitation, Limnology and Oceanography, 49, 1582–1592, doi:10.4319/lo.2004.49.5.1582, https://aslopubs.onlinelibrary.wiley.com/doi/abs/10.4319/lo.2004.49.5.1582, 2004.

Krom, M. D., Emeis, K.-C., and Van Cappellen, P.: Why is the Eastern Mediterranean phosphorus limited?, Progress in Oceanography, 85, 236–244, doi:10.1016/j.pocean.2010.03.003, http://www.sciencedirect.com/science/article/pii/S0079661110000340, 2010.

Lascaratos, A., Roether, W., Nittis, K., and Klein, B.: Recent changes in deep water formation and spreading in the eastern Mediterranean Sea: a review, Progress in Oceanography, 44, 5–36, doi:10.1016/S0079-6611(99)00019-1, http://www.sciencedirect.com/science/article/pii/S0079661199000191, 1999.

970 Lazzari, P., Mattia, G., Solidoro, C., Salon, S., Crise, A., Zavatarelli, M., Oddo, P., and Vichi, M.: The impacts of climate change and environmental management policies on the trophic regimes in the Mediterranean Sea: Scenario analyses, Journal of Marine Systems, 135, 137–149, doi:10.1016/j.jmarsys.2013.06.005, http://linkinghub.elsevier.com/retrieve/pii/S0924796313001425, 2014.

Lefort, S., Aumont, O., Bopp, L., Arsouze, T., Gehlen, M., and Maury, O.: Spatial and body-size dependent
975 response of marine pelagic communities to projected global climate change, Global Change Biology, 21, 154–164, doi:10.1111/gcb.12679, http://onlinelibrary.wiley.com/doi/10.1111/gcb.12679/abstract, 2015.

Locarnini, R. A., Garcia, H. E., Boyer, T. P., Antonov, J. I., and Levitus, S.: World Ocean Atlas 2005, Volume 3: Dissolved Oxygen, Apparent Oxygen Utilization, and Oxygen Saturation [+DVD], NOAA Atlas NESDIS, http://www.vliz.be/nl/imis?module=ref&refid=117383&printversion=1&dropIMIStitle=1, 2006.

980 Ludwig, W., Dumont, E., Meybeck, M., and Heussner, S.: River discharges of water and nutrients to the Mediterranean and Black Sea: Major drivers for ecosystem changes during past and future decades?, Progress in Oceanography, 80, 199–217, doi:10.1016/j.pocean.2009.02.001, http://linkinghub.elsevier.com/retrieve/pii/S0079661109000020, 2009.

Ludwig, W., Bouwman, A. F., Dumont, E., and Lespinas, F.: Water and nutrient fluxes from major Mediterranean
985 ranean and Black Sea rivers: Past and future trends and their implications for the basin-scale budgets, Global Biogeochemical Cycles, 24, GB0A13, doi:10.1029/2009GB003594, http://onlinelibrary.wiley.com/doi/10.1029/2009GB003594/abstract, 2010.

Luna, G. M., Bianchelli, S., Decembrini, F., Domenico, E. D., Danovaro, R., and Dell'Anno, A.: The dark portion of the Mediterranean Sea is a bioreactor of organic matter cycling, Global Biogeochemical Cycles,
990 26, doi:10.1029/2011GB004168, https://agupubs.onlinelibrary.wiley.com/doi/abs/10.1029/2011GB004168, 2012.

Macias, D. M., Garcia-Gorriz, E., and Stips, A.: Productivity changes in the Mediterranean Sea for the twenty-first century in response to changes in the regional atmospheric forcing, Frontiers in Marine Science, 2, doi:10.3389/fmars.2015.00079, https://www.frontiersin.org/articles/10.3389/fmars.2015.00079/full, 2015.

995 Madec, G.: NEMO ocean engine, http://eprints.soton.ac.uk/64324/, 2008.

Marty, J.-C., Chiavérini, J., Pizay, M. D., and Avril, B.: Seasonal and interannual dynamics of nutrients and phytoplankton pigments in the western Mediterranean Sea at the DYFAMED time-series station (1991-1999), Deep-Sea Research, Part II. Topical Studies in Oceanography, http://www.vliz.be/en/imis?module=ref&refid=39389&printversion=1&dropIMIStitle=1, 2002.

1000 Monod, J.: Recherches sur la croissance des cultures bactériennes, Hermann, 1958.

Morel, A. and Gentili, B.: Yellow substance and the shades of blue in the Mediterranean Sea, Biogeosciences Discussions, 6, 8503–8530, http://adsabs.harvard.edu/abs/2009BGD.....6.8503M, 2009.

Moutin, T., Van Wambeke, F., and Prieur, L.: Introduction to the Biogeochemistry from the Oligotrophic to the Ultraoligotrophic Mediterranean (BOUM) experiment, Biogeosciences, 9, 3817–3825, doi:10.5194/bg-
1005 9-3817-2012, http://www.biogeosciences.net/9/3817/2012/, 2012.

Nabat, P., Somot, S., Mallet, M., Sevault, F., Chiacchio, M., and Wild, M.: Direct and semi-direct aerosol radiative effect on the Mediterranean climate variability using a coupled regional climate system model, Climate Dynamics, 44, 1127–1155, doi:10.1007/s00382-014-2205-6, https://link.springer.com/article/10.1007/s00382-014-2205-6, 2015.

1010 Nittis, K., Lascaratos, A., and Theocharis, A.: Dense water formation in the Aegean Sea: Numerical simulations during the Eastern Mediterranean Transient, Journal of Geophysical Research: Oceans, 108, 8120, doi:10.1029/2002JC001352, http://onlinelibrary.wiley.com/doi/10.1029/2002JC001352/abstract, 2003.

Palmieri, J., Orr, J. C., Dutay, J.-C., Béranger, K., Schneider, A., Beuvier, J., and Somot, S.: Simulated anthropogenic CO2 storage and acidification of the Mediterranean Sea, Biogeosciences, 12, 781–802,

1015 doi:10.5194/bg-12-781-2015, http://www.biogeosciences.net/12/781/2015/, 2015.

Powley, H. R., Dürr, H. H., Lima, A. T., Krom, M. D., and Van Cappellen, P.: Direct Discharges of Domestic Wastewater are a Major Source of Phosphorus and Nitrogen to the Mediterranean Sea, https://core.ac.uk/display/74234820, 2016.

Powley, H. R., Krom, M. D., and Cappellen, P. V.: Understanding the unique biogeochemistry of the

1020 Mediterranean Sea: Insights from a coupled phosphorus and nitrogen model, Global Biogeochemical Cycles, 31, 1010–1031, doi:10.1002/2017GB005648, https://agupubs.onlinelibrary.wiley.com/doi/abs/10.1002/2017GB005648, 2017.

Pujo-Pay, M., Conan, P., Oriol, L., Cornet-Barthaux, V., Falco, C., Ghiglione, J.-F., Goyet, C., Moutin, T., and Prieur, L.: Integrated survey of elemental stoichiometry (C, N, P) from the western to eastern Mediterranean

1025 Sea, Biogeosciences, 8, 883–899, doi:10.5194/bg-8-883-2011, http://www.biogeosciences.net/8/883/2011/, 2011.

Redfield, A. C., Ketchum, B. H., and Richards, F. A.: The influence of organisms on the composition of seawater, The sea: ideas and observations on progress in the study of the seas, http://www.vliz.be/en/imis?module=ref&refid=28944&printversion=1&dropIMIStitle=1, 1963.

1030 Richon, C., Dutay, J.-C., Dulac, F., Wang, R., Balkanski, Y., Nabat, P., Aumont, O., Desboeufs, K., Laurent, B., Guieu, C., Raimbault, P., and Beuvier, J.: Modeling the impacts of atmospheric deposition of nitrogen and desert dust–derived phosphorus on nutrients and biological budgets of the Mediterranean Sea, Progress in Oceanography, doi:10.1016/j.pocean.2017.04.009, http://www.sciencedirect.com/science/article/pii/S0079661116301811, 2017.

1035 Richon, C., Dutay, J.-C., Dulac, F., Wang, R., and Balkanski, Y.: Modeling the biogeochemical impact of atmospheric phosphate deposition from desert dust and combustion sources to the Mediterranean Sea, Biogeosciences, 15, 2499–2524, doi:10.5194/bg-15-2499-2018, https://www.biogeosciences.net/15/2499/2018/, 2018.

Robinson, A. R., Leslie, W. G., Theocharis, A., and Lascaratos, A.: Mediterranean Sea Circulation, in:

1040 Encyclopedia of Ocean Sciences (Second Edition), edited by Steele, J. H., pp. 710–725, Academic Press, Oxford, doi:10.1016/B978-012374473-9.00376-3, http://www.sciencedirect.com/science/article/pii/B9780123744739003763, 2001.

Rodellas, V., Garcia-Orellana, J., Masqué, P., Feldman, M., and Weinstein, Y.: Submarine groundwater discharge as a major source of nutrients to the Mediterranean Sea, Proceedings of the National Academy of

1045 Sciences, 112, 3926–3930, doi:10.1073/pnas.1419049112, http://www.pnas.org/content/112/13/3926, 2015.

Roether, W., Klein, B., and Hainbucher, D.: The Eastern Mediterranean Transient, in: The Mediterranean Sea, edited by Borzelli, G. L. E., Gačić, M., Lionello, P., and Paolalanotte-Rizzoli, pp. 75–83, John Wiley & Sons, Inc., http://onlinelibrary.wiley.com/doi/10.1002/9781118847572.ch6/summary, 2014.

Rohling, E. J.: Shoaling of the Eastern Mediterranean Pycnocline due to reduction of excess evaporation: Implications for sapropel formation, Paleoceanography, 6, 747–753, doi:10.1029/91PA02455, http://onlinelibrary.wiley.com/doi/10.1029/91PA02455/abstract, 1991.

Rohling, E. J.: Review and new aspects concerning the formation of eastern Mediterranean sapropels, Marine Geology, 122, 1–28, doi:10.1016/0025-3227(94)90202-X, http://www.sciencedirect.com/science/article/pii/002532279490202X, 1994.

Rossignol-Strick, M., Nesteroff, W., Olive, P., and Vergnaud-Grazzini, C.: After the deluge: Mediterranean stagnation and sapropel formation, Nature, 295, 105–110, doi:10.1038/295105a0, http://www.nature.com/nature/journal/v295/n5845/abs/295105a0.html, 1982.

Royer, J.-F., Cariolle, D., Chauvin, F., Déqué, M., Douville, H., Hu, R.-M., Planton, S., Rascol, A., Ricard, J.-L., Salas Y Melia, D., Sevault, F., Simon, P., Somot, S., Tyteca, S., Terray, L., and Valcke, S.: Simulation des changements climatiques au cours du XXIe siècle incluant l'ozone stratosphérique, Comptes Rendus Geoscience, 334, 147–154, doi:10.1016/S1631-0713(02)01728-5, http://www.sciencedirect.com/science/article/pii/S1631071302017285, 2002.

Ruti, P. M., Somot, S., Giorgi, F., Dubois, C., Flaounas, E., Obermann, A., Dell'Aquila, A., Pisacane, G., Harzallah, A., Lombardi, E., Ahrens, B., Akhtar, N., Alias, A., Arsouze, T., Aznar, R., Bastin, S., Bartholy, J., Béranger, K., Beuvier, J., Bouffies-Cloché, S., Brauch, J., Cabos, W., Calmanti, S., Calvet, J.-C., Carillo, A., Conte, D., Coppola, E., Djurdjevic, V., Drobinski, P., Elizalde-Arellano, A., Gaertner, M., Galàn, P., Gallardo, C., Gualdi, S., Goncalves, M., Jorba, O., Jordà, G., L'Heveder, B., Lebeaupin-Brossier, C., Li, L., Liguori, G., Lionello, P., Maciàs, D., Nabat, P., Önol, B., Raikovic, B., Ramage, K., Sevault, F., Sannino, G., Struglia, M. V., Sanna, A., Torma, C., and Vervatis, V.: Med-CORDEX Initiative for Mediterranean Climate Studies, Bulletin of the American Meteorological Society, 97, 1187–1208, doi:10.1175/BAMS-D-14-00176.1, http://journals.ametsoc.org/doi/10.1175/BAMS-D-14-00176.1, 2016.

Sanchez-Gomez, E., Somot, S., and Mariotti, A.: Future changes in the Mediterranean water budget projected by an ensemble of regional climate models, Geophysical Research Letters, 36, L21 401, doi:10.1029/2009GL040120, http://onlinelibrary.wiley.com/doi/10.1029/2009GL040120/abstract, 2009.

Santinelli, C., Ibello, V., Lavezza, R., Civitarese, G., and Seritti, A.: New insights into C, N and P stoichiometry in the Mediterranean Sea: The Adriatic Sea case, Continental Shelf Research, 44, 83–93, doi:10.1016/j.csr.2012.02.015, http://www.sciencedirect.com/science/article/pii/S0278434312000519, 2012.

Schaap, D. M. and Lowry, R. K.: SeaDataNet – Pan-European infrastructure for marine and ocean data management: unified access to distributed data sets, International Journal of Digital Earth, 3, 50–69, doi:10.1080/17538941003660974, http://www.tandfonline.com/doi/abs/10.1080/17538941003660974, 2010.

Sevault, F., Somot, S., Alias, A., Dubois, C., Lebeaupin-Brossier, C., Nabat, P., Adloff, F., Déqué, M., and Decharme, B.: A fully coupled Mediterranean regional climate system model: design and evaluation of the

1085   ocean component for the 1980–2012 period, Tellus A, 66, doi:10.3402/tellusa.v66.23967, http://www.tellusa. net/index.php/tellusa/article/view/23967, 2014.

Somot, S., Sevault, F., and Déqué, M.: Transient climate change scenario simulation of the Mediterranean Sea for the twenty-first century using a high-resolution ocean circulation model, Climate Dynamics, 27, 851–879, doi:10.1007/s00382-006-0167-z, http://link.springer.com/10.1007/s00382-006-0167-z, 2006.

1090   Soto-Navarro, J., Somot, S., Sevault, F., Beuvier, J., Criado-Aldeanueva, F., García-Lafuente, J., and Béranger, K.: Evaluation of regional ocean circulation models for the Mediterranean Sea at the Strait of Gibraltar: volume transport and thermohaline properties of the outflow, Climate Dynamics, 44, 1277–1292, doi:10.1007/s00382-014-2179-4, https://link.springer.com/article/10.1007/s00382-014-2179-4, 2015.

Spillman, C. M., Imberger, J., Hamilton, D. P., Hipsey, M. R., and Romero, J. R.: Modelling the effects of Po 1095   River discharge, internal nutrient cycling and hydrodynamics on biogeochemistry of the Northern Adriatic Sea, Journal of Marine Systems, 68, 167–200, doi:10.1016/j.jmarsys.2006.11.006, http://www.sciencedirect. com/science/article/pii/S0924796306003459, 2007.

Takahashi, T., Broecker, W. S., and Langer, S.: Redfield ratio based on chemical data from isopycnal surfaces, Journal of Geophysical Research: Oceans (1978–2012), 90, 6907–6924, doi:10.1029/JC090iC04p06907, 1100   http://onlinelibrary.wiley.com/doi/10.1029/JC090iC04p06907/abstract, 1985.

Taylor, K. E., Stouffer, R. J., and Meehl, G. A.: An Overview of CMIP5 and the Experiment Design, Bulletin of the American Meteorological Society, 93, 485–498, doi:10.1175/BAMS-D-11-00094.1, http://journals. ametsoc.org/doi/abs/10.1175/BAMS-D-11-00094.1, 2012.

Theocharis, A., Nittis, K., Kontoyiannis, H., Papageorgiou, E., and Balopoulos, E.: Climatic changes in 1105   the Aegean Sea influence the eastern Mediterranean thermohaline circulation (1986–1997), Geophysical Research Letters, 26, 1617–1620, doi:10.1029/1999GL900320, http://onlinelibrary.wiley.com/doi/10.1029/ 1999GL900320/abstract, 1999.

Vadsaria, T., Ramstein, G., Li, L., and Dutay, J.-C.: Sensibilité d'un modèle océan-atmosphère (LMDz-NEMOMED8) à un flux d'eau douce : cas du dernier épisode de sapropèle en mer Méditerranée, Quaternaire, 1110   28, 2017.

Velaoras, D. and Lascaratos, A.: North-Central Aegean Sea surface and intermediate water masses and their role in triggering the Eastern Mediterranean Transient, Journal of Marine Systems, 83, 58–66, doi:10.1016/j.jmarsys.2010.07.001, wOS:000282548300005, 2010.

Yogev, T., Rahav, E., Bar-Zeev, E., Man-Aharonovich, D., Stambler, N., Kress, N., Béjà, O., Mulholland, 1115   M. R., Herut, B., and Berman-Frank, I.: Is dinitrogen fixation significant in the Levantine Basin, East Mediterranean Sea?, Environmental Microbiology, 13, 854–871, doi:10.1111/j.1462-2920.2010.02402.x, http://onlinelibrary.wiley.com/doi/10.1111/j.1462-2920.2010.02402.x/abstract, 2011.

Name	Dynamics (NEMO years)	Buffer zone concentrations	River inputs
CTRL	1966–1981	1966–1981	1966–1981
CTRL_R	1966–1981	1966–1981	1980–2099
CTRL_RG	1966–1981	1980–2099	1980–2099
HIS/A2	1980–2099	1980–2099	1980–2099

Table 1. Description of the simulations. The years indicate the forcing years throughout the 120 years of simulation. The cycles are repeated in the CTRL simulations.

Simulation	Period	Whole Med.	Western	Eastern	Ionian-Levantine	Adriatic	Aegean	Atlantic buffer zon
	1980–1999	551	241	310	305	1.5	4.0	535
HIS/A2	2030–2049	570 (+3.4)	240 (0)	329 (+6.1)	324 (+6.2)	1.4 (0)	3.6 (-10)	543 (+1.5)
	2080–2099	598 (+8.5)	251 (+4.1)	346 (+11.6)	341 (+11.8)	1.5 (0)	3.5 (-12.5)	562 (+5.0)
	1980–1999	545	238	307	302	1.6	4.0	532
CTRL	2030–2049	553 (+1.5)	238 (0)	314 (+2.3)	309 (+2.3)	1.6 (0)	4.2 (+5.0)	532 (0)
	2080-2099	560 (+2.6)	241 (+1.3)	319 (+3.9)	313 (+3.6)	1.7 (+6.3)	4.2 (+5.0)	532 (0)
	1980–1999	547	239	309	303	1.5	4.2	534
CTRL_R	2030-2049	536 (-2.0)	232 (-2.9)	304 (-1.6)	299 (-1.3)	1.4 (-6.7)	3.5 (-17)	534 (0)
	2080-2099	538 (-1.6)	230 (-3.8)	309 (0)	303 (0)	1.5 (0)	3.7 (-12)	534 (0)
	1980–1999	548	239	309	303	1.5	4.2	535
CTRL_RG	2030–2049	536 (-2.2)	233 (-2.5)	303 (-1.9)	298 (-1.7)	1.4 (-6.7)	3.5 (-17)	544 (+1.7)
	2080–2099	540 (-1.5)	235 (-1.7)	306 (-1.0)	301 (-0.7)	1.4 (-6.7)	3.6 (-14)	562 (+5.0)

Table 2. Simulated integrated phosphate content (10^9 mol) over 20 years periods in the Mediterranean sub–basins in the different simulations. Basins are the same as defined in Fig.2 of Adloff et al. (2015), with the eastern basin including the Ionian, Levantine, Adriatic and Aegean subbasins. Values in parenthesis indicate the percentage difference from the 1980–1999 period.

1120

Simulation	Period	Whole Med.	Western	Eastern	Ionian-Levantine	Adriatic	Aegean	Atlantic buffer zo
	1980–1999	13400	5520	7890	7690	66.9	132	8091
HIS/A2	2030–2049	13800 (+3.0)	5450 (-1.3)	8350 (+5.8)	8100 (+5.3)	88.5 (+32)	163 (+23)	8230 (+1.7)
	2080–2099	14700 (+9.7)	5750 (+4.2)	8920 (+13)	8650 (+12)	98.3 (+47)	164 (+24)	8510 (+5.2)
	1980–1999	13500	5530	7970	7760	66.2	144	8050
CTRL	2030–2049	12900 (-4.4)	5320 (-3.8)	7610 (-4.5)	7420 (-4.4)	61.7 (-6.8)	131 (-9.0)	8050 (0)
	2080-2099	12500 (-7.4)	5170 (-6.5)	7330 (-8.0)	7150 (-7.9)	58.7 (-11)	123 (-15)	8050 (0)
	1980–1999	13300	5470	7870	7760	66.8	138	8070
CTRL_R	2030-2049	13300 (0)	5250 (-4.0)	8020 (+1.9)	7770 (+0.1)	88.0 (+32)	162 (+17)	8070 (0)
	2080-2099	13700 (+3.0)	5300 (-3.1)	8440 (+7.2)	8170 (+5.3)	94.2 (+41)	177 (+28)	8080 (+0.1)
	1980–1999	13300	5480	7870	7760	66.8	138	8090
CTRL_RG	2030–2049	13300 (0)	5270 (-3.8)	8010 (+1.8)	7760 (0)	88.0 (+32)	162 (+17)	8080 (-0.1)
	2080–2099	13800 (+3.8)	5390 (-1.6)	8430 (+7.1)	8160 (+5.2)	94.3 (+41)	177 (+28)	8080 (-0.1)

Table 3. Simulated integrated nitrate content (10^9 mol) over 20 years periods in the Mediterranean sub–basins in the different simulations. Basins are the same as defined in Fig.2 of Adloff et al. (2015), with the eastern basin including the Ionian, Levantine, Adriatic and Aegean subbasins. Values in parenthesis indicate the percentage difference from the 1980–1999 period.

Simulation	Period	Whole Med.	Western	Eastern	Ionian-Levantine	Adriatic	Aegean	Atlantic buffer
	1980–1999	25700	9680	16000	13500	830	1720	3210
HIS/A2	2030–2049	23800 (-7.4)	8980 (-7.2)	14800 (-7.5)	12700 (-5.9)	720 (-13)	1440 (-16)	3280 (+2.2)
	2080–2099	23400 (-8.9)	9180 (-5.1)	14300 (-11)	12200 (-9.6)	690 (-17)	1390 (-19)	3570 (+11)
	1980–1999	27000	10200	16700	14200	880	1670	3180
CTRL	2030–2049	27000 (0)	10200 (0)	16900 (+1.2)	14300 (+0.7)	890 (+1.1)	1710 (+2.4)	3180 (0)
	2080-2099	26600 (-1.5)	9980 (-2.2)	16600 (-0.1)	14000 (-1.4)	880 (0)	1690 (+1.2)	3180 (0)
	1980–1999	27000	10300	16700	14100	875	1720	3210
CTRL_R	2030-2049	26800 (-0.7)	10100 (-1.9)	16700 (0)	14300 (+1.4)	780 (-12)	1610 (-6.4)	3210 (0)
	2080-2099	26400 (-2.2)	9940 (-3.5)	16500 (-1.2)	14100 (0)	760 (-13)	1600 (-7.0)	3220 (0.3)
	1980–1999	27000	10300	16700	14100	875	1720	3230
CTRL_RG	2030–2049	26900 (-0.4)	10200 (-1.0)	16700 (0)	14300 (+1.4)	780 (-12)	1600 (-7.0)	3260 (+0.9)
	2080–2099	26700 (-1.1)	10200 (-1.0)	16500 (-1.2)	14100 (0)	750 (-14)	1600 (-7.0)	3420 (+5.9)

Table 4. Simulated integrated chlorophyll production (10^9 mol) over 20 years periods in the Mediterranean sub–basins in the different simulations. Basins are the same as defined in Fig.2 of Adloff et al. (2015), with the eastern basin including the Ionian, Levantine, Adriatic and Aegean subbasins. Values in parenthesis indicate the percentage difference from the 1980–1999 period.
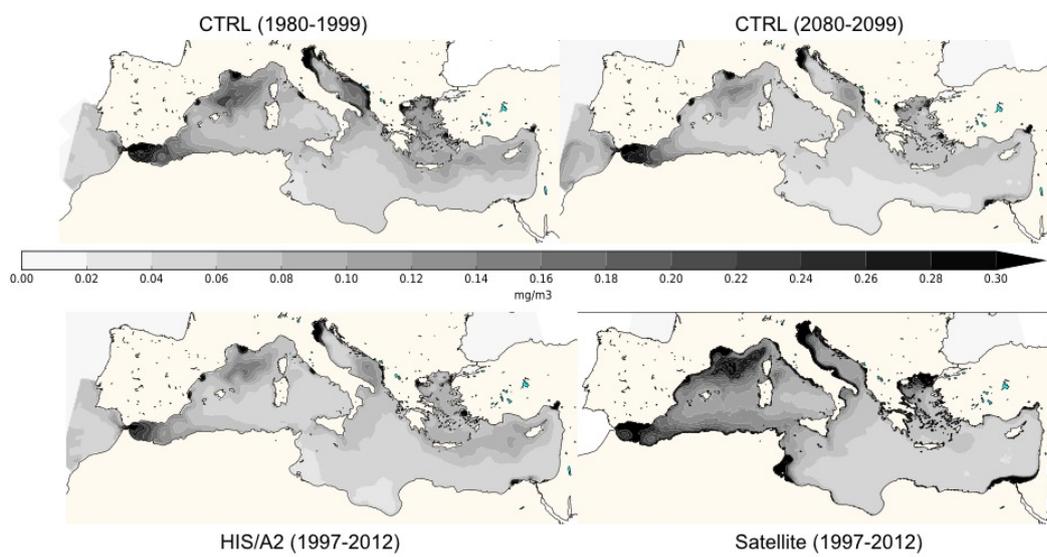
Figure 1. Average surface chlorophyll concentration from the CTRL (top, left: 1980–1999 right: 2080–2099) and HIS/A2 (bottom left) simulations, and from satellite estimations (MyOcean Dataset 1997–2012, bottom right).
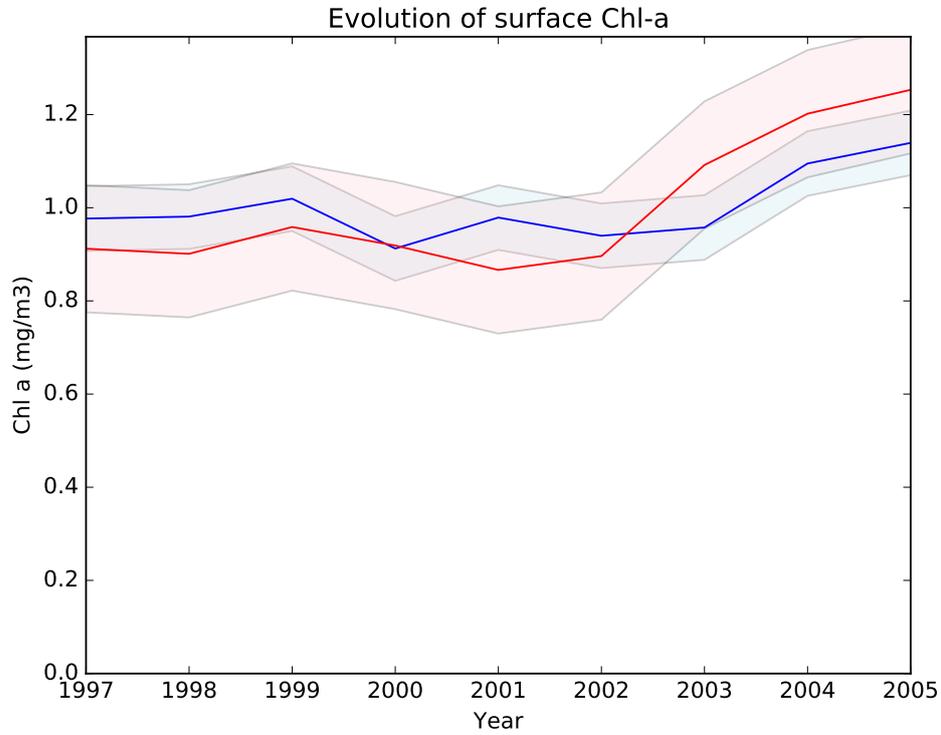
Figure 2. Average surface chlorophyll concentration from the HIS/A2 simulation in blue and from the SeaW-iFs satellite data (Bosc et al., 2004) in red over the period 1997–2005. Shaded colors represent the standard deviations. Values are normalized by dividing by the average cholorphyll concentration over the period.

(a) Average Mediterranean SST   (b) Average Mediterranean SSS
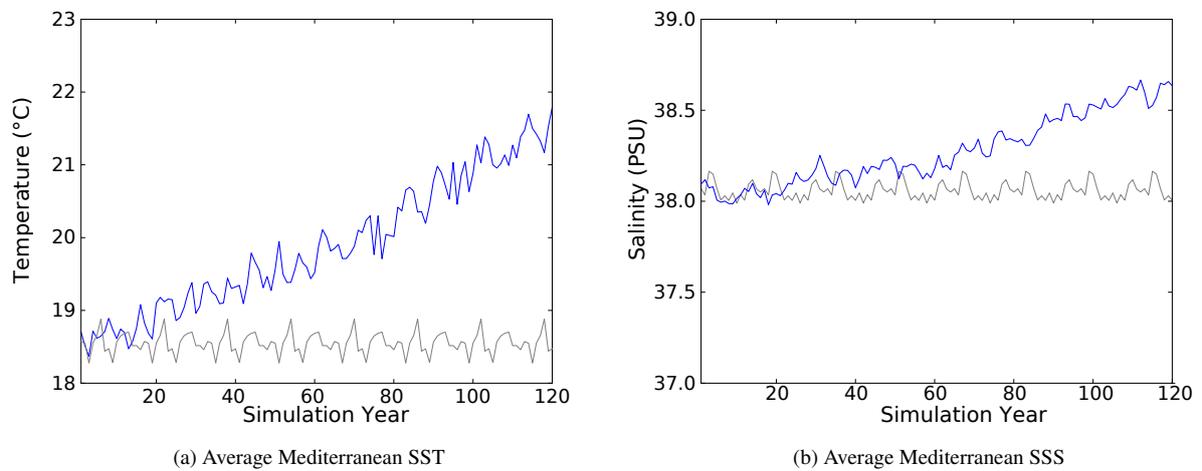
Figure 3. Evolution of average Mediterranean SST (left) and SSS (right) in CTRL (grey line) and HIS/A2 (blue line) simulations.
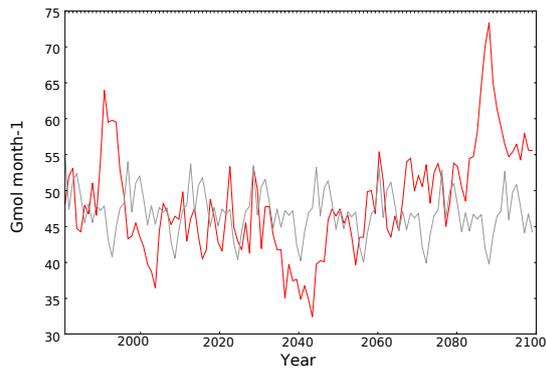
(a) Total incoming nitrate
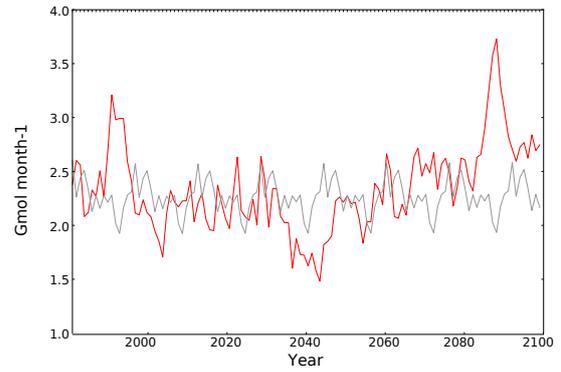
(b) Total incoming phosphate
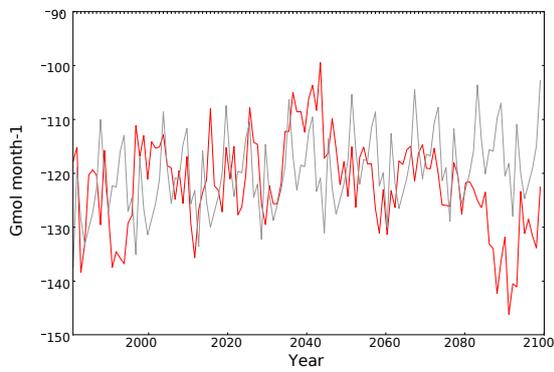
(c) Total outgoing nitrate
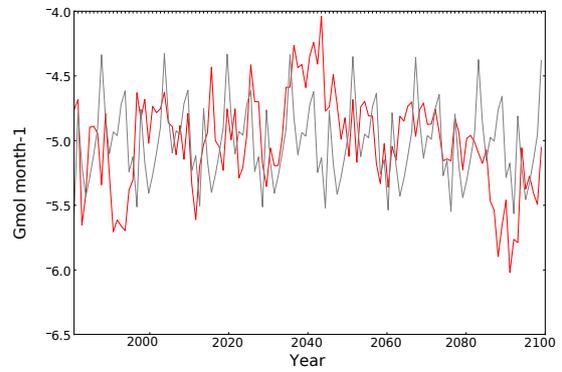
(d) Total outgoing phosphate

Figure 4. Evolution of total incoming (top) and outgoing (bottom) fluxes of nitrate and phosphate (10^9 mol month^{-1}) through the Strait of Gibraltar in CTRL (grey line) and HIS/A2 (red line). Negative values indicate outgoing fluxes of nutrients.
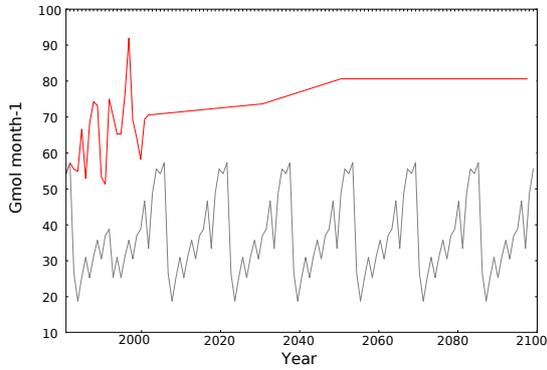
(a) Total river discharge of nitrate
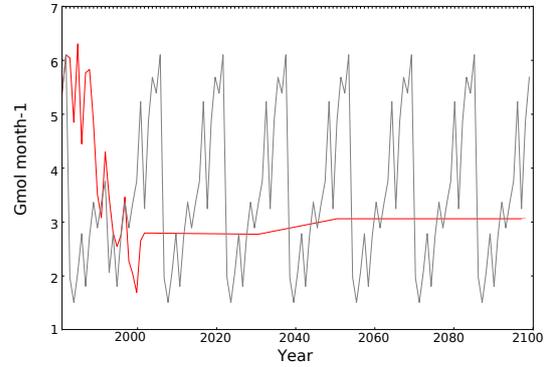
(b) Total river discharge of phosphate

Figure 5. Evolution of total river discharge fluxes of nitrate and phosphate (10^9mol month^{-1}) to the Mediterranean Sea in CTRL (grey line) and HIS/A2 (red line).
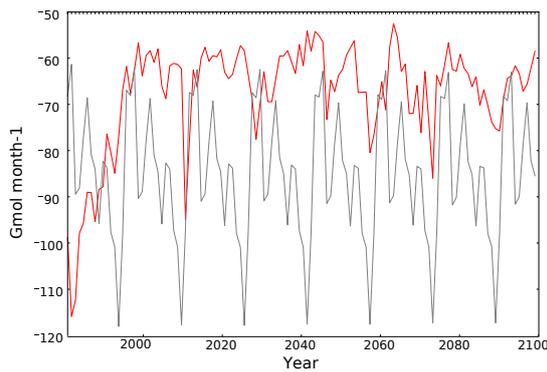
(a) Total nitrogen sedimentation
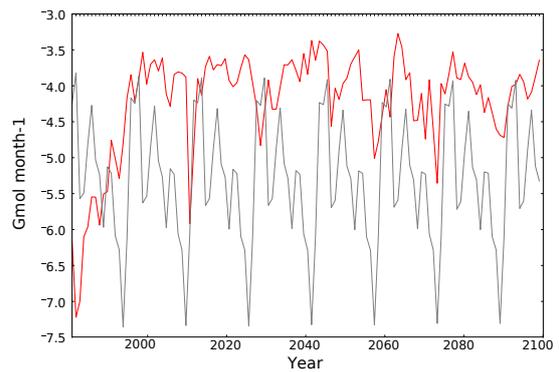
(b) Total phosphorus sedimentation

Figure 6. Evolution of total sedimentation fluxes of N and P (10^9mol month^{-1}) in the Mediterranean Sea in CTRL (grey line) and HIS/A2 (red line). Negative fluxes indicate that the nutrients are exiting the Mediterranean waters.

(a) phosphate surface (0–200 m) (b) phosphate intermediate (200–600 m) (c) phosphate deep (600 m–bottom)

(d) phosphate surface (0–200 m) (e) phosphate intermediate (200–600 m) (f) phosphate deep (600 m–bottom)
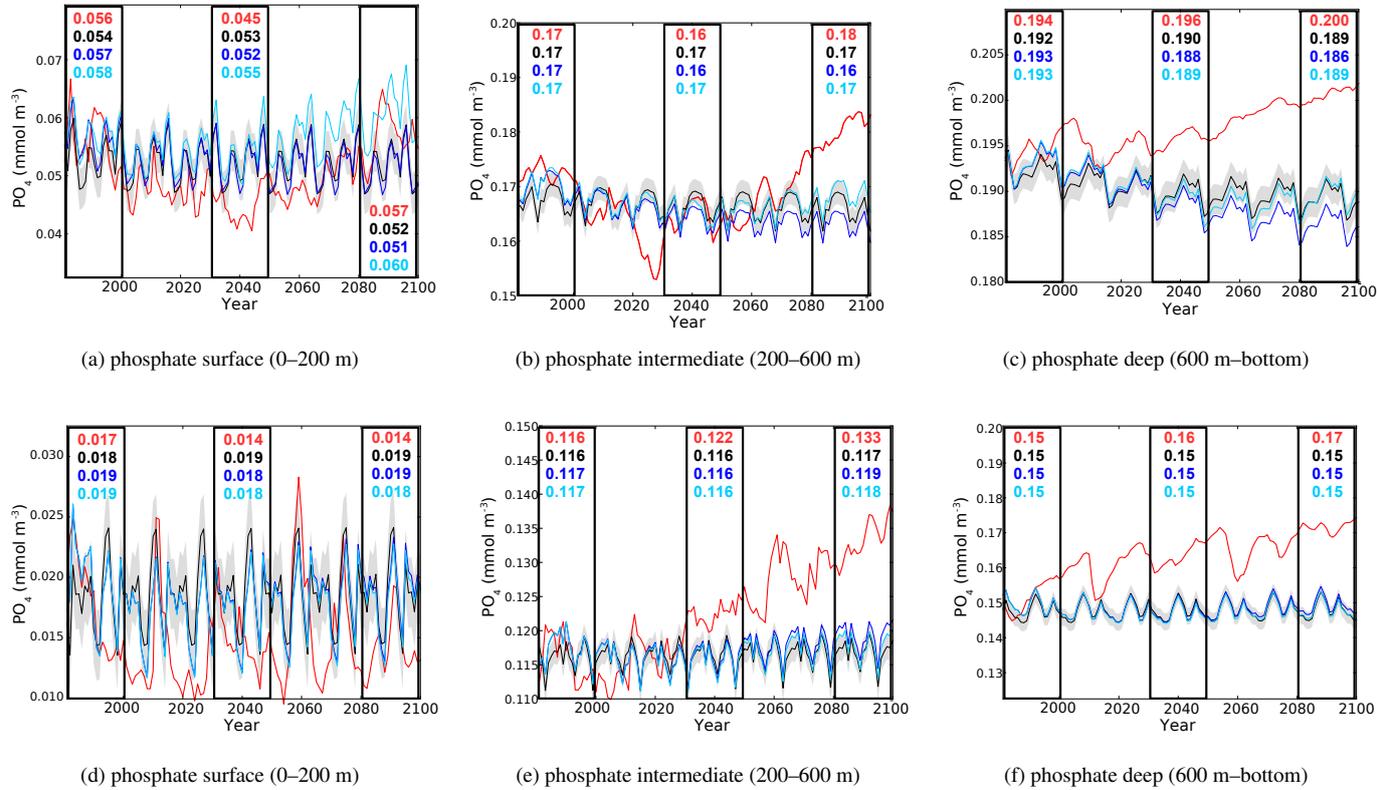
Figure 7. Evolution of yearly average phosphate concentration (10^{-3} mol m^{-3}) in the surface (left), intermediate (middle) and bottom (right) layers in the western (top) and eastern (bottom) basin. Red lines represent the HIS/A2 simulation, black lines represent the CTRL (with standard deviation), blue and light blue lines represent the CTRL_R and CTRL_RG simulations respectively. Colored numbers in the highlighted areas represent the average concentrations in the corresponding simulations for the highlighted time periods.
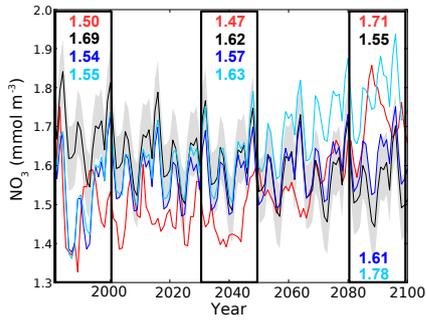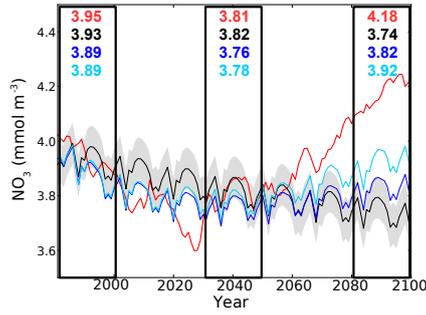
(a) nitrate surface (0–200 m)   (b) nitrate intermediate (200–600 m)   (c) nitrate deep (600 m–bottom)
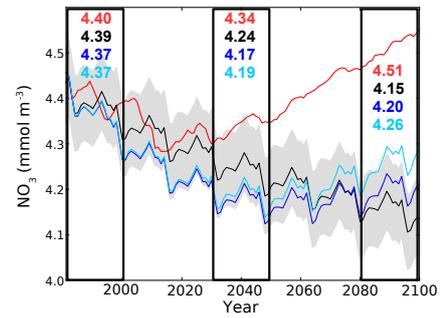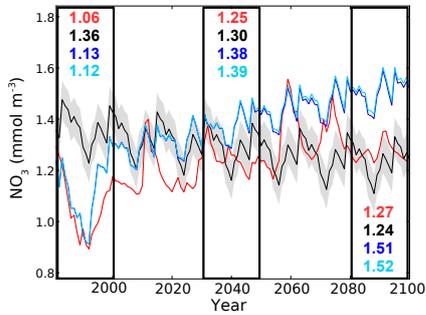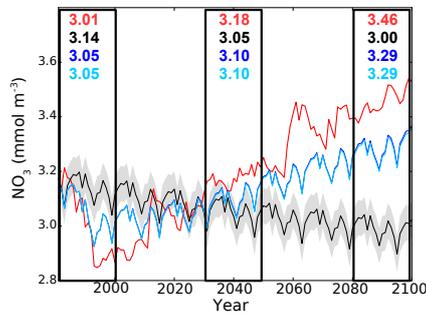
(d) nitrate surface (0–200 m)   (e) nitrate intermediate (200–600 m)   (f) nitrate deep (600 m–bottom)
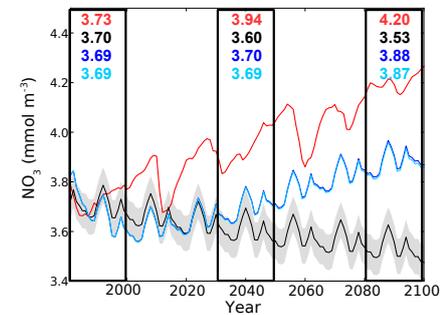
Figure 8. Evolution of yearly average nitrate concentration (10^{-3} mol m^{-3}) in the surface (left), intermediate (middle) and bottom (right) layers in the western (top) and eastern (bottom) basins. Red lines represent the HIS/A2 simulation, black lines represent the CTRL (with standard deviation), blue and light blue lines represent the CTRL_R and CTRL_RG simulations respectively. Colored numbers in the highlighted areas represent the average concentrations in the corresponding simulations for the highlighted time periods.
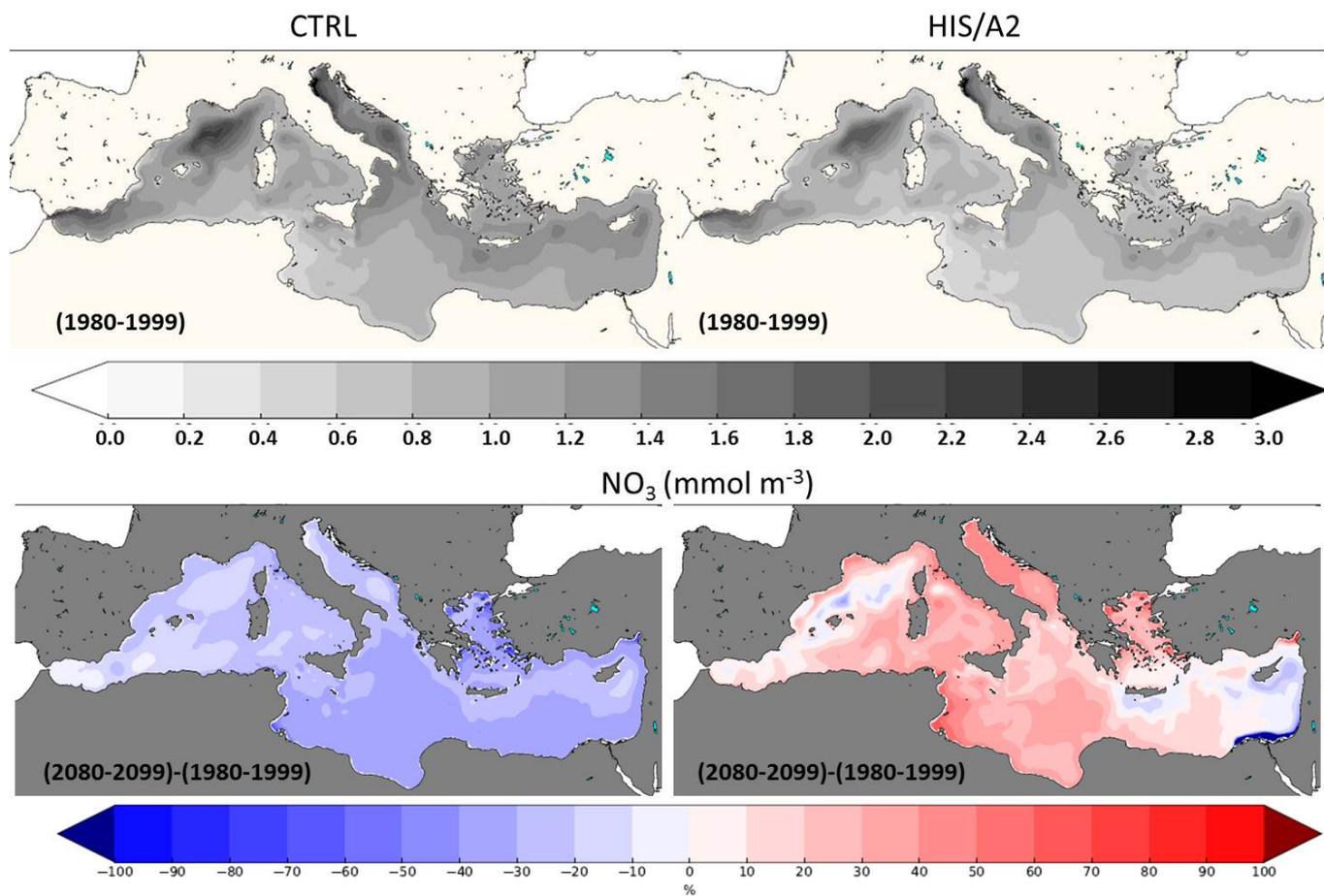
Figure 9. Present (1980–1999, top) interannual average surface (0–200 m) concentrations of nitrate (10^{-3} mol m^{-3}) in the CTRL (left) HIS/A2 (right) simulations. The bottom maps show the relative difference (in %) between the 2080–2099 and the 1980–1999 periods in CTRL (left) and HIS/A2 (right).
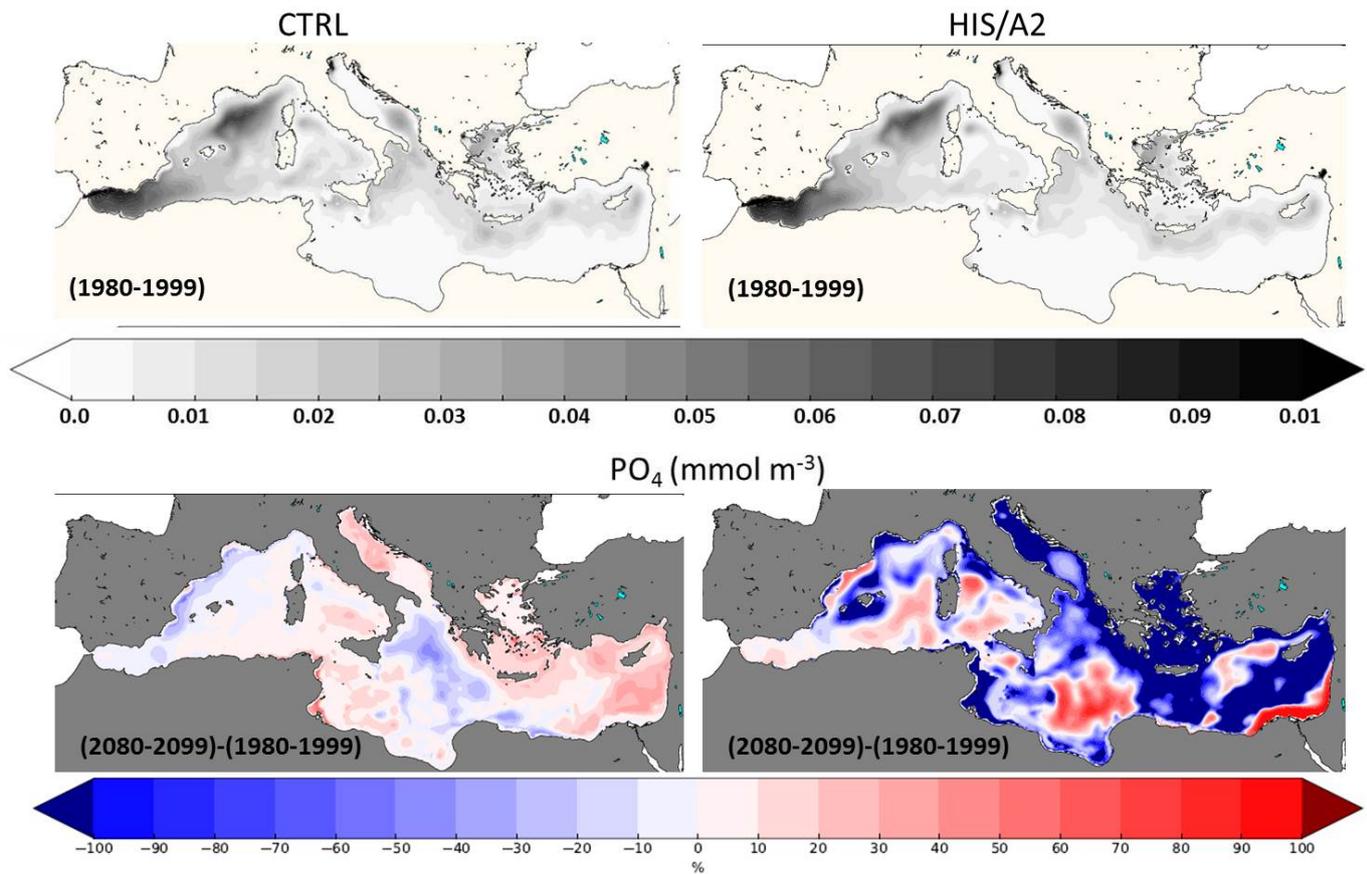
Figure 10. Present (1980–1999, top) interannual average surface (0–200m) concentrations of phosphate $(10^{-3}$ mol m$^{-3})$ in the CTRL (left) and HIS/A2 (right) simulations. The bottom maps show the relative difference (in %) in primary production between the 2080–2099 and the 1980–1999 periods in CTRL (left) and HIS/A2 (right).
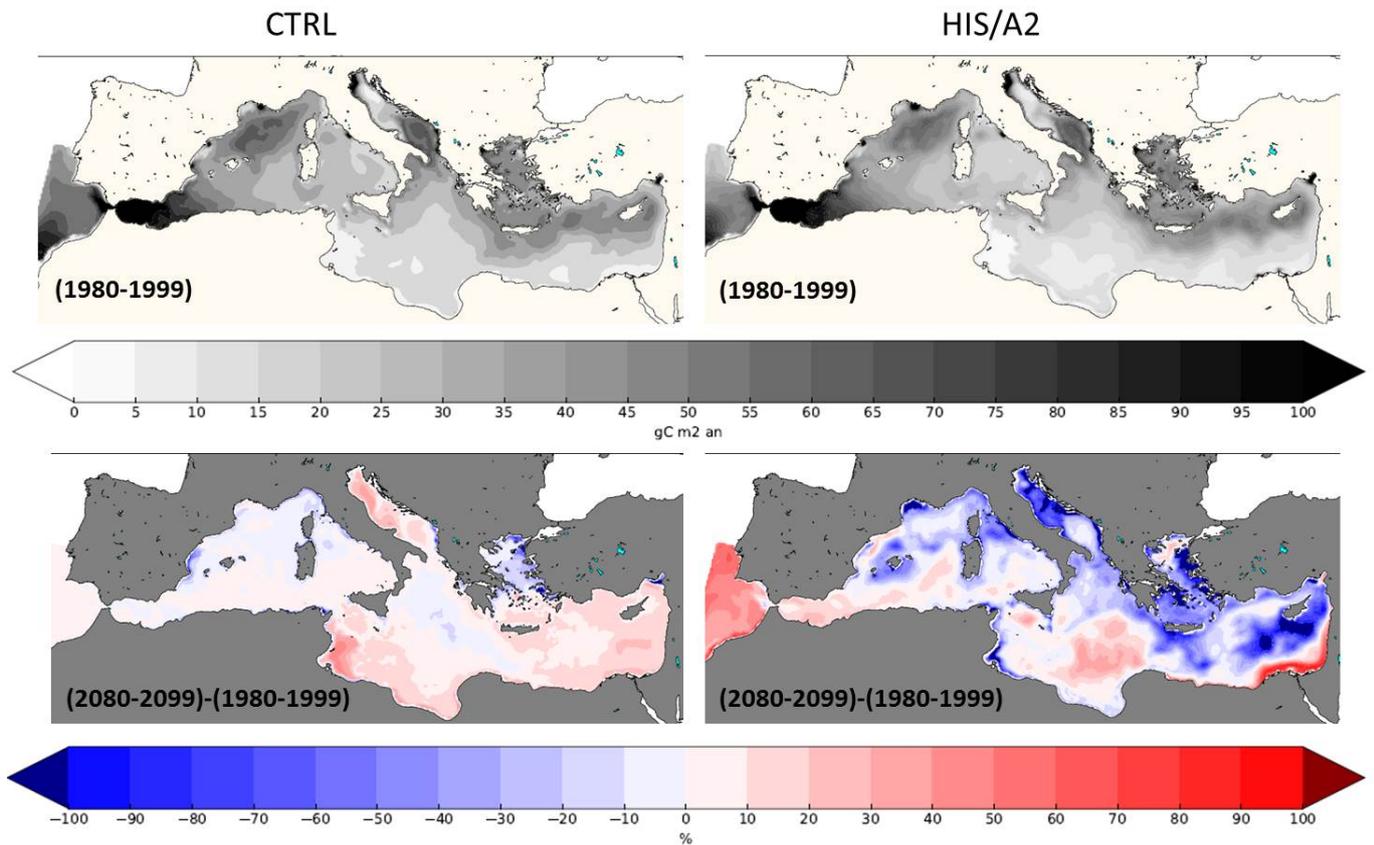
Figure 11. Present (1980–1999, top) interannual average surface (0–200 m) integrated primary production (gC m^{-2}) in the CTRL (left) and HIS/A2 (right) simulations. The bottom maps show the relative difference (in %) between the 2080–2099 and the 1980–1999 periods in CTRL (left) and HIS/A2 (right).
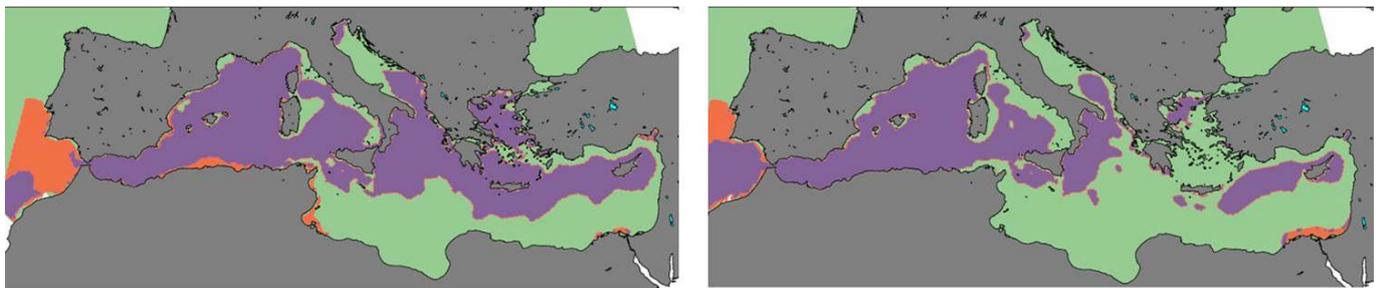
Figure 12. Present (1980–1999) and future (2080-2099) interannual average surface (0–200 m) limiting nutrient in the HIS/A2 simulation. N and P colimitation is considered when limitation factors for N and P differ by less than 1 %. Green zones are P–limited, Orange zones are N–Limited and purple zones are N and P co–limited.
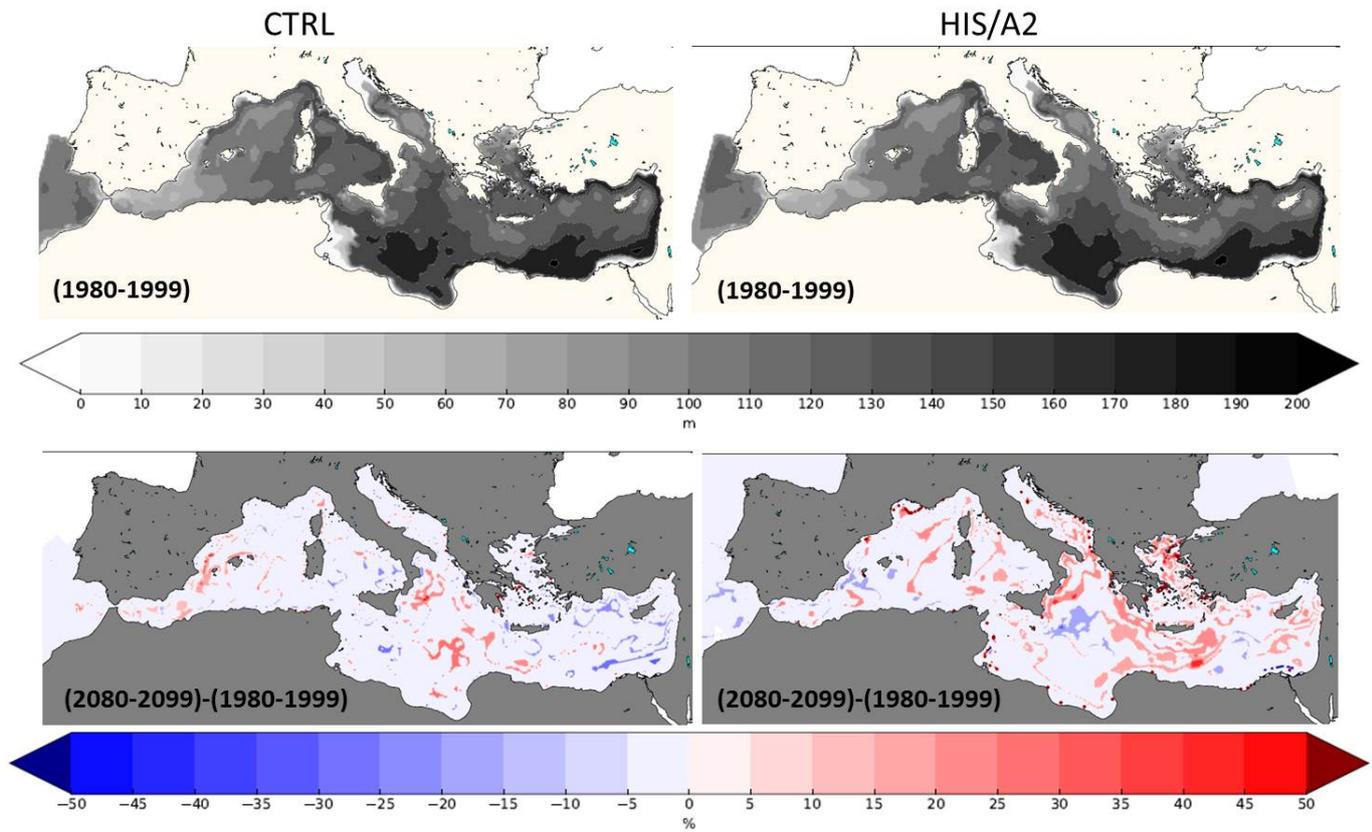
Figure 13. Present (1980–1999, top) interannual average DCM (m) in the CTRL (left) and HIS/A2 (right) simulations. The bottom maps show the relative difference (in %) in DCM between the 2080–2099 and the 1980–1999 periods in CTRL (left) and HIS/A2 (right).
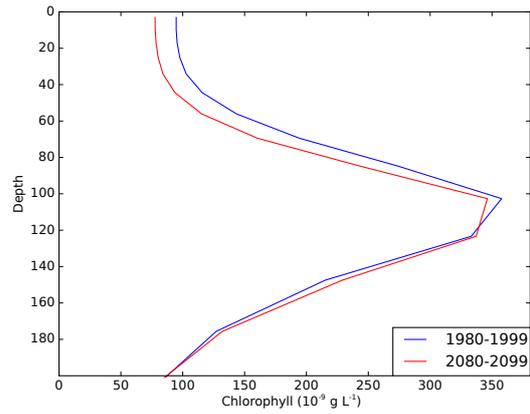
(a) DYFAMED
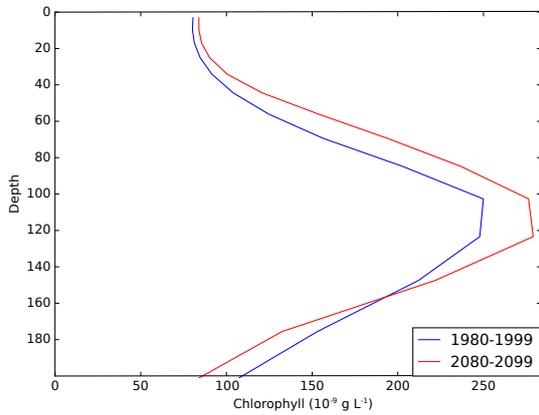
(b) Western basin
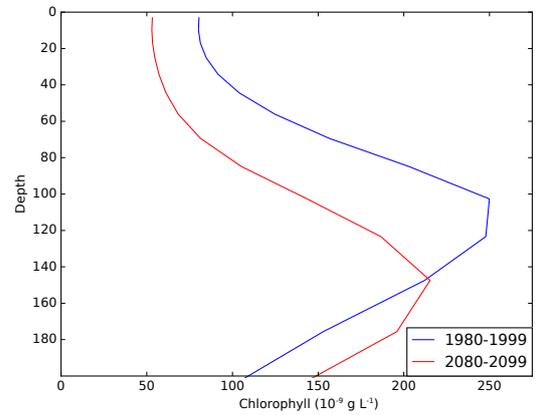
(c) Eastern basin

Figure 14. Present (1980–1999) and future (2080–2099) interannual average vertical profiles of total chlorophyll a ($10e^{-9}$g L^{-1}) at the DYFAMED station and averaged profiles over the western and eastern (including Aegean and Adriatic) basins.
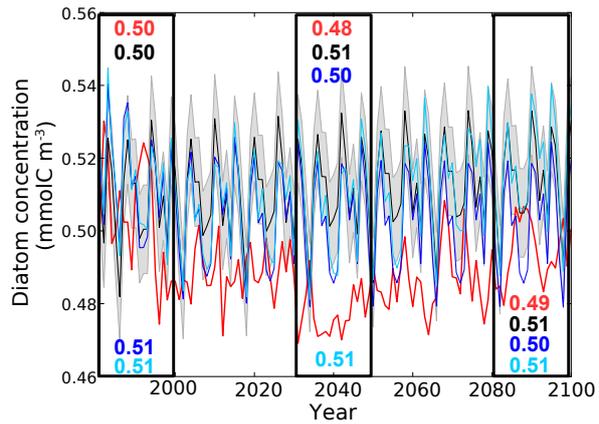
(a) Nanophytoplankton western basin
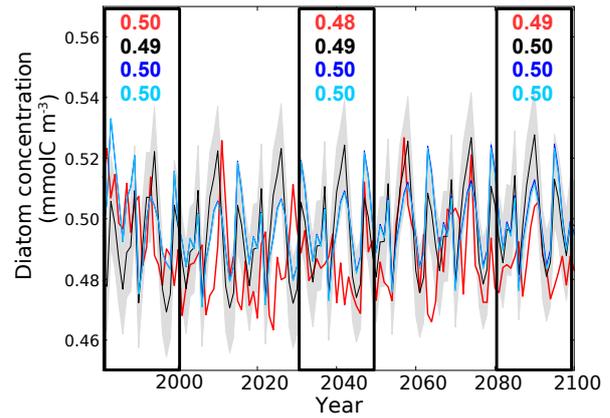
(b) Nanophytoplankton eastern basin
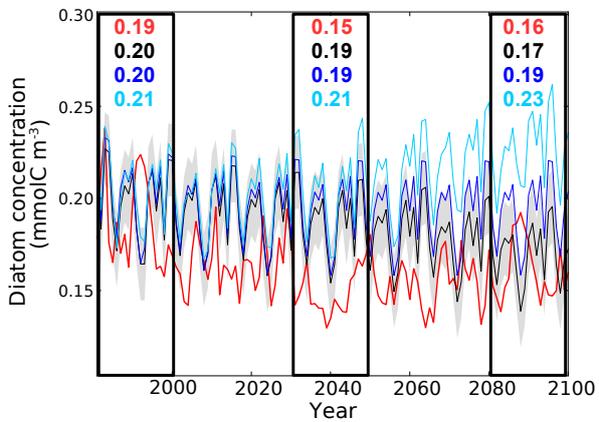
(c) Diatoms western basin
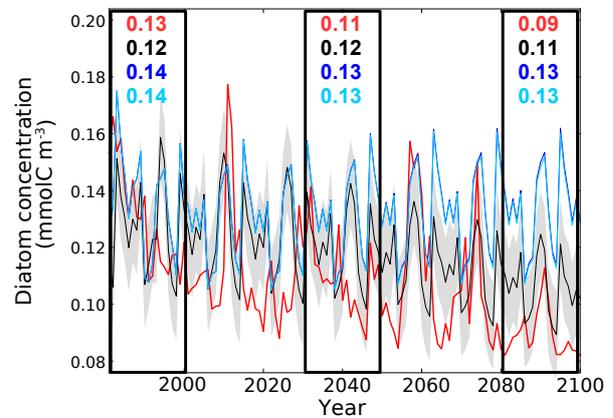
(d) Diatoms eastern basin

Figure 15. Evolution of yearly average nanophytoplankton and diatoms concentration (10^{-3}mol m^{-3}) in the surface layer of the western and eastern basin. Red line represent the HIS/A2 simulation, black lines represent the CTRL (with standard deviation), blue and light blue lines represent the CTRL_R and CTRL_RG simulations respectively. Colored numbers in the highlighted areas represent the average concentrations in the corresponding simulations for the highlighted time periods.
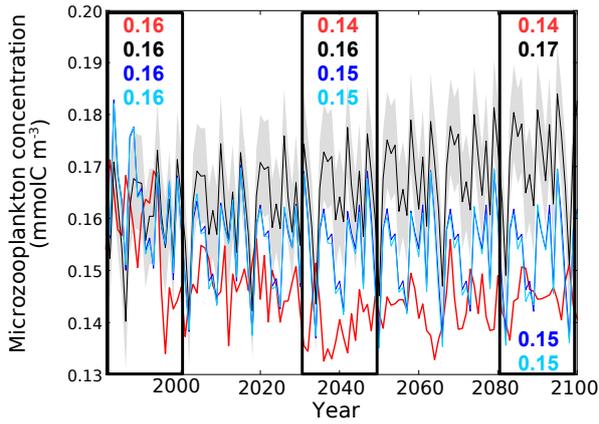
(a) Microzooplankton western basin
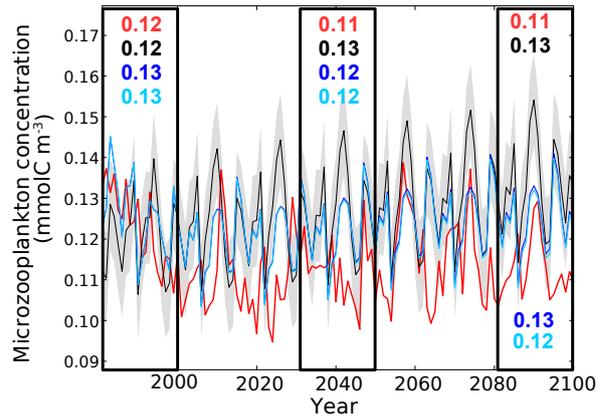
(b) Microzooplankton eastern basin
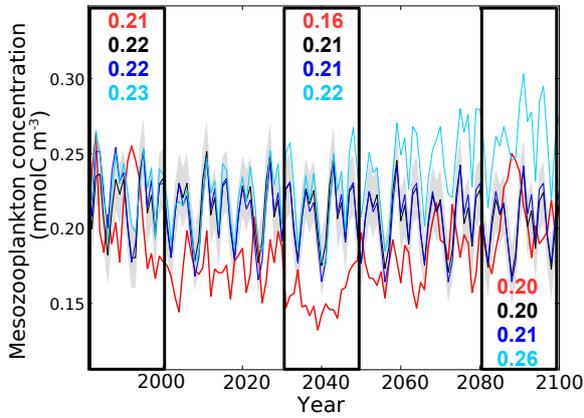
(c) Mesozooplankton western basin
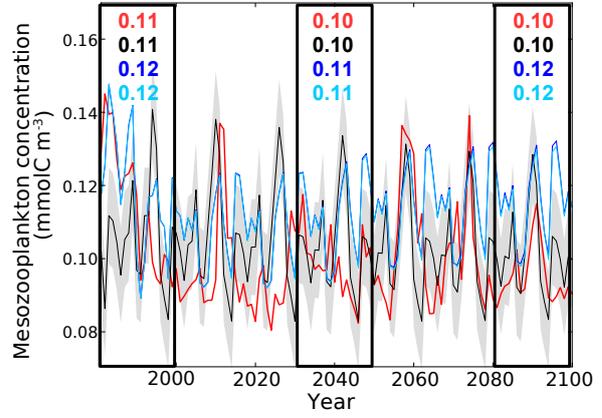
(d) Mesozooplankton eastern basin

Figure 16. Evolution of yearly average microzooplankton and mesozooplankton concentrations (10^{-3}mol m^{-3}) in the surface layer of the western and eastern basins. Red lines represent the HIS/A2 simulation, black lines represent the CTRL (with standard deviation), blue and light blue lines represent the CTRL_R and CTRL_RG simulations respectively. Colored numbers in the highlighted areas represent the average concentrations in the corresponding simulations for the corresponding time periods.
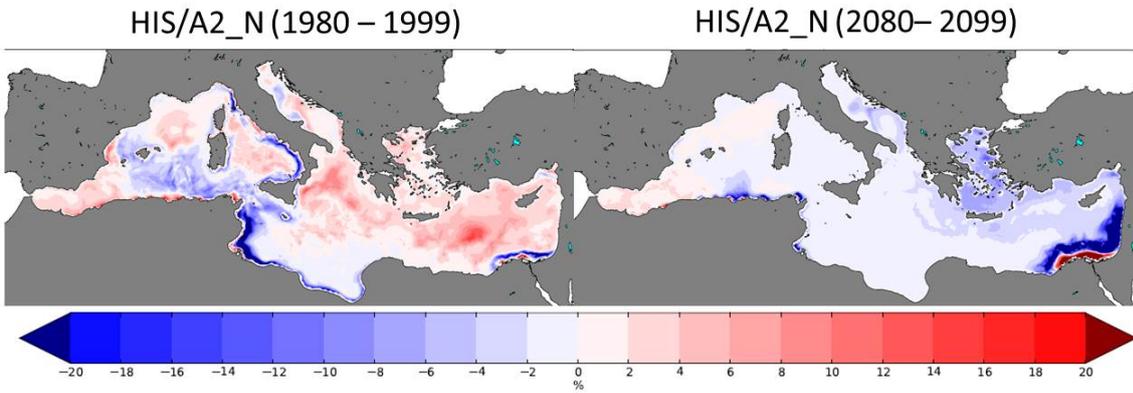
(a) Relative effects of total nitrogen deposition
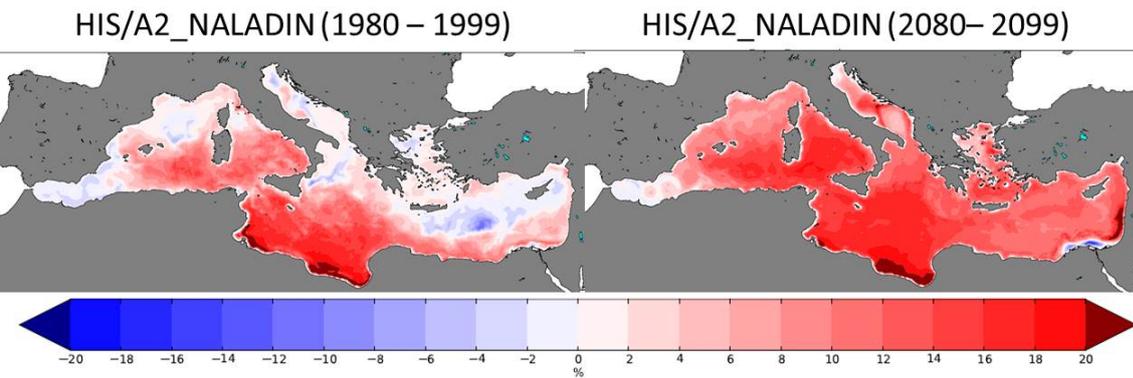
(b) Relative effects of natural dust deposition

Figure 17. Present (1980–1999) and future (2080–2099) relative effects of total nitrogen (top) and natural dust (bottom) deposition on surface (0–10 m) total primary production.
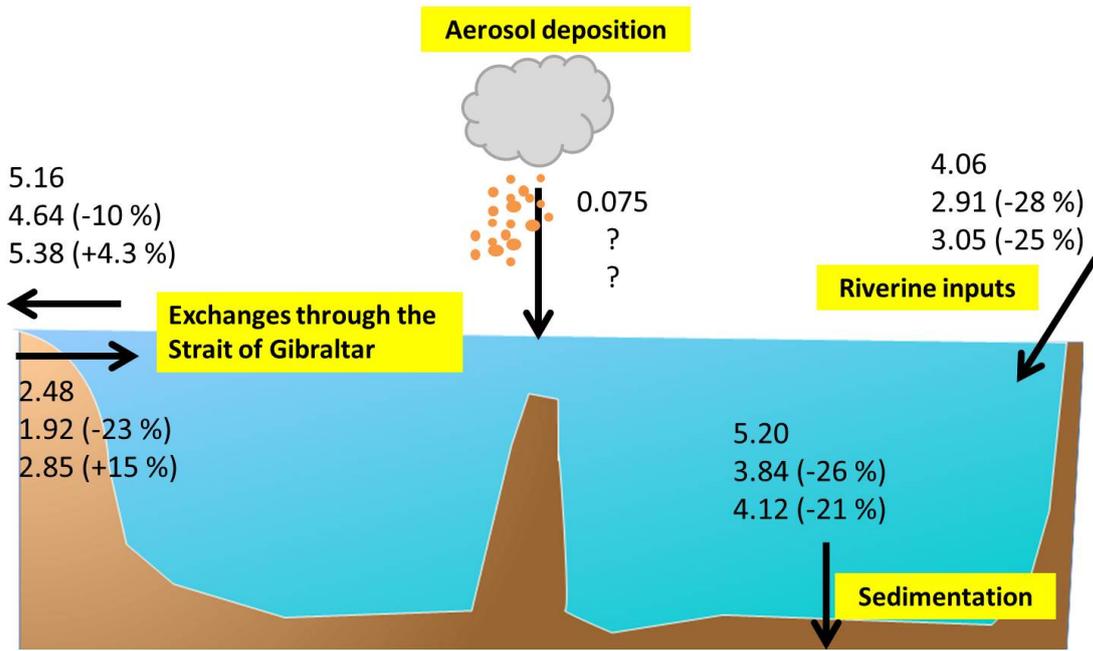
(a) Phosphate fluxes
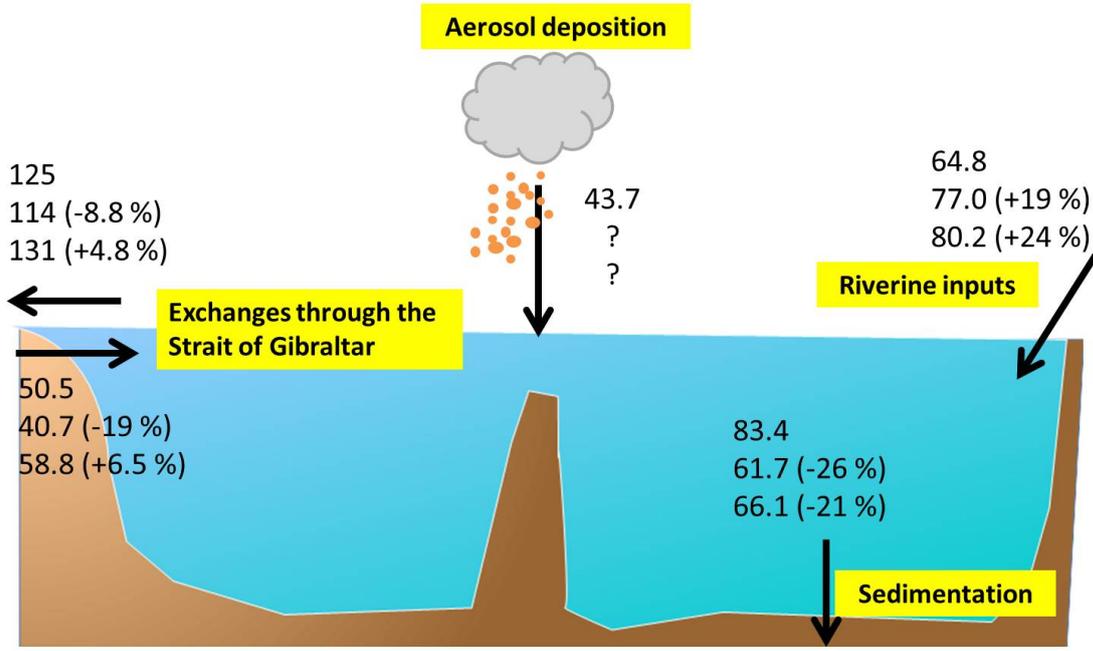
(b) Nitrate fluxes

Figure 18. Schematic diagrams illustrating the Mediterranean budgets of phosphate and nitrate. For each component, the 3 lines represent the average fluxes (in Gmol year^{-1}) over the periods 1980–1999, 2030-2049 and 2080-2099, numbers in parenthesis indicate the percentage difference from the 1980–1999 values.

(a) February

(b) May
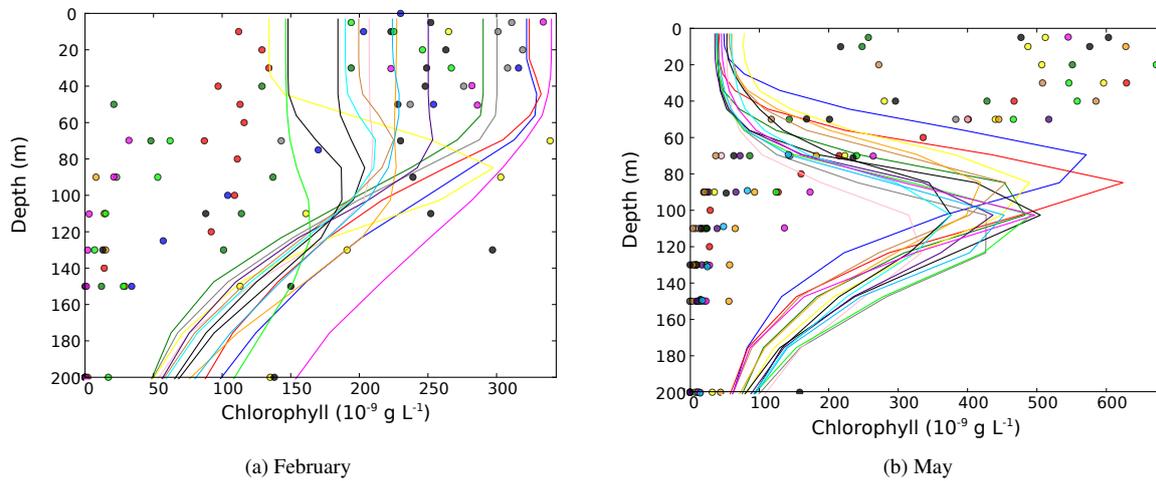
Figure A1. Average chlorophyll–a profiles in February (left) and May (right) for the years 1991 to 2005 at the DYFAMED station in the Ligurian Sea Sea (43.4277°N, 7.2522°E). Dots represent data points (Marty et al., 2002; Faugeras et al., 2003). Lines represent the HIS/A2 simulation. Colors represent individual years.


(a) Phosphate
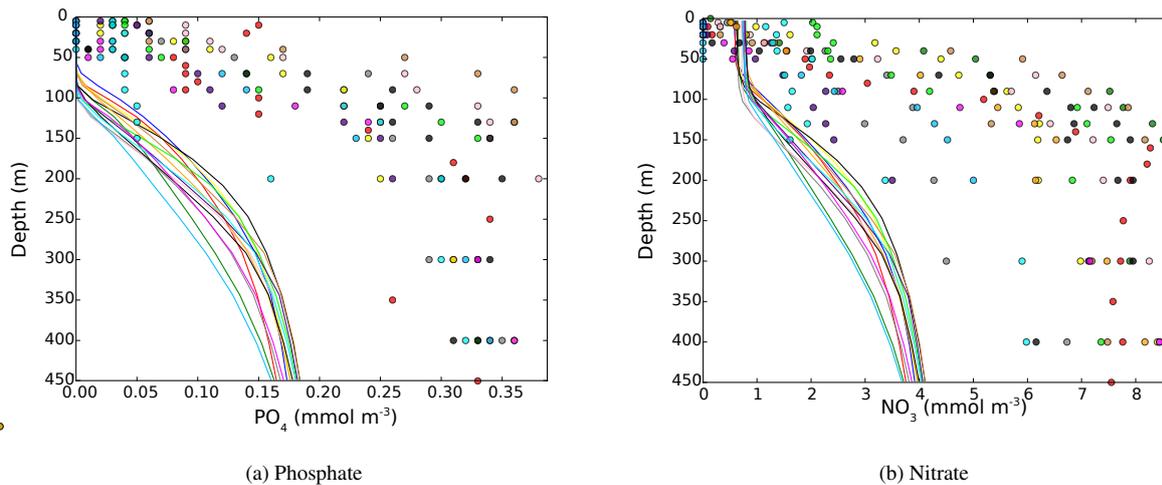
(b) Nitrate

Figure A2. Average phosphate (left) and nitrate (right) profiles in May for the years 1991 to 2005 at the DY-FAMED station in the Ligurian Sea Sea (43.4277°N, 7.2522°E). Dots represent data points (Marty et al., 2002; Faugeras et al., 2003). Lines represent the HIS/A2 simulation. Colors represent individual years.
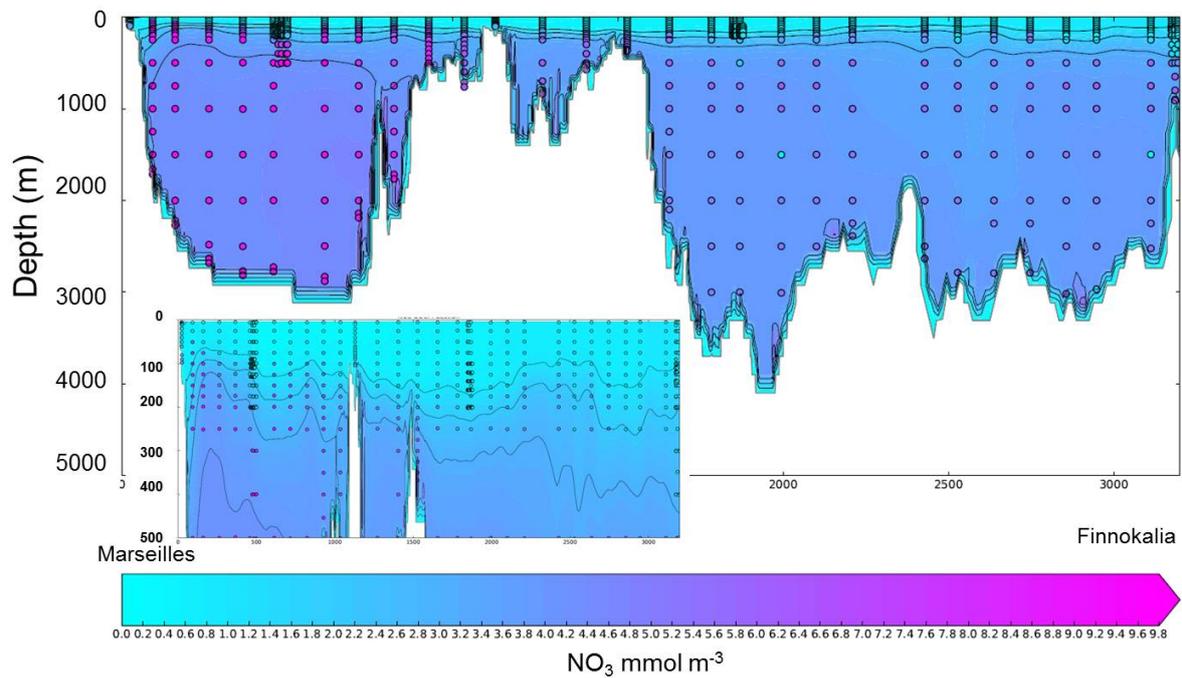
(a) nitrate concentration
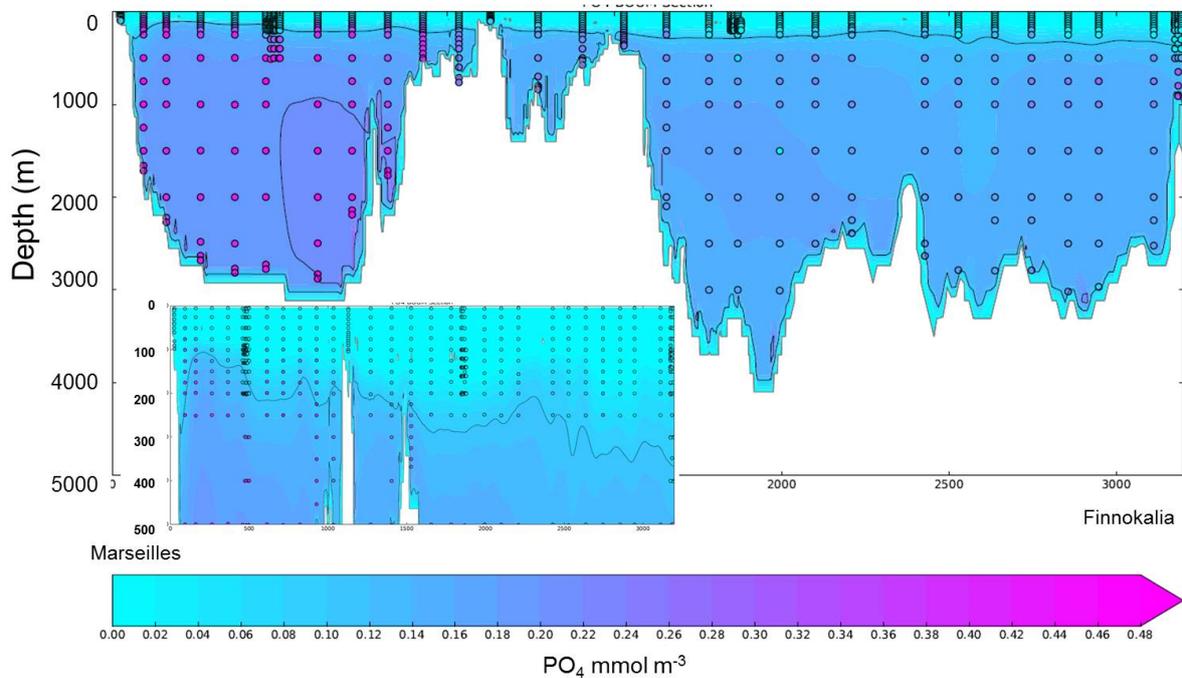
(b) PO$_4$ concentration

Figure A3. Average concentrations of nitrate (top) and phosphate (bottom) for the 20 first years of the control simulation (CTRL). The dots represent data along a transect from Marseille to Finokalia from the BOUM campaign (distances in km Moutin et al., 2012). The framed areas represent a vertical zoom of the top 500 m along the whole transect.